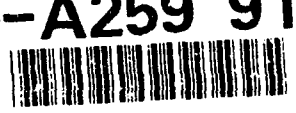

ARI-RR-964

GAS PHASE KINETIC MODELING AND SENSITIVITY ANALYSIS OF B/H/O/C/F COMBUSTION SYSTEMS

Prepared by

R.C. Brown and C.E. Kolb
Center for Environmental and Atmospheric Physics
Aerodyne Research, Inc.
45 Manning Road
Billerica, MA 01821

R.A. Yetter and F.L. Dryer,
Department of Mechanical and Aerospace Engineering
Princeton University
Princeton, NJ 08514

H. Rabitz
Department of Chemistry
Princeton University
Princeton, NJ 08814

Prepared for

R.S. Miller
Mechanics Division
Office of Naval Research
800 Quincy Street
Arlington, VA 22217

January 1993

REPORT DOCUMENTATION PAGE

Form Approved
OMB No. 0704-0188

1. AGENCY USE ONLY (Leave blank)	2. REPORT DATE	3. REPORT TYPE AND DATES COVERED
	January 28, 1993	Final Report June 26,1991-June 28,1992

4. TITLE AND SUBTITLE

Gas Phase Kinetic Modeling and Sensitivity Analysis of B/H/O/C/F Combustion Systems

5. FUNDING NUMBERS

6. AUTHOR(S)

R.C. Brown and C.E. Kolb, Aerodyne Research, Inc.
R.A. Yetter and F.L. Dryer Princeton University

7. PERFORMING ORGANIZATION NAME(S) AND ADDRESS(ES)

Aerodyne Research, Inc.
45 Manning Road
Billerica, MA 01821

8. PERFORMING ORGANIZATION REPORT NUMBER

ARI-RR-964

9. SPONSORING/MONITORING AGENCY NAME(S) AND ADDRESS(ES)

Office of Naval Research
800 Quincy Street
Arlington, VA 22217

10. SPONSORING/MONITORING AGENCY REPORT NUMBER

N00014-91-C-0141

11. SUPPLEMENTARY NOTES

12a. DISTRIBUTION/AVAILABILITY STATEMENT

Distribution unlimited; approval for public release

12b. DISTRIBUTION CODE

13. ABSTRACT (Maximum 200 words)

A kinetic model is presented to describe the high temperature, gas phase B/H/O/C/F chemistry associated with fluoroamino/nitroamino/B(s) mixtures. The results of thermodynamic constant temperature and pressure calculations for a prototypical fluoroamino/nitroamino based oxidizer and solid boron are presented to characterize the equilibrium speciation under boron rich and boron lean conditions. Based on an analysis of the predicted equilibrium speciation, key gas phase reactants are selected and a reaction mechanism describing potential reaction pathways is formulated. Rate parameters for elementary reactions were obtained from published experimental/theoretical data or estimated using transisition state arguments and scaling relations. The results of kinetic calculations for several isothermal and adiabatic systems are presented which illustrate the general high temperature mechanistic behavior of B/H/O/C/F systems. Standard reaction flux/pathway and gradient sensitivity analysis techniques are used to identify important reaction pathways.

14. SUBJECT TERMS

Boron, kinetic model, sensitivity analysis, combustion

15. NUMBER OF PAGES

73

16. PRICE CODE

17. SECURITY CLASSIFICATION OF REPORT	18. SECURITY CLASSIFICATION OF THIS PAGE	19. SECURITY CLASSIFICATION OF ABSTRACT	20. LIMITATION OF ABSTRACT
Unclassified	Unclassified	Unclassified	

ABSTRACT

A kinetic model is presented to describe the high temperature, gas phase B/H/O/C/F chemistry associated with fluoroamino/nitroamino/B(s) mixtures. The results of thermodynamic constant temperature and pressure calculations for a prototypical fluoroamino/nitroamino based oxidizer and solid boron are presented to characterize the equilibrium speciation under boron rich and boron lean conditions. Based on an analysis of the predicted equilibrium speciation, key gas phase reactants are selected and a reaction mechanism describing potential reaction pathways is formulated. Rate parameters for elementary reactions were obtained from published experimental/theoretical data or estimated using transition state arguments and scaling relations. The results of kinetic calculations for several isothermal and adiabatic systems are presented which illustrate the general high temperature mechanistic behavior of B/H/O/C/F systems. Standard reaction flux/pathway and gradient sensitivity analysis techniques are used to identify important reaction pathways.

TABLE OF CONTENTS

Section		Page
	Abstract	ii
	Table of Contents	iii
	List of Figures	iv
	List of Tables	viii
	Executive Summary	ix
1.0	INTRODUCTION	1-1
2.0	THERMOCHEMISTRY	2-1
	2.1 Oxidizer/Fuel Mixture Composition	2-1
	2.2 Equilibrium Calculations Overview	2-2
	2.3 F-HMX/TMETN Mixture	2-4
	2.4 F-HMX/TMETN/B(s) Mixtures	2-5
3.0	REACTION MECHANISM	3-1
	3.1 Gas Phase Reactants	3-1
	3.2 B/H/O/C/F Kinetics	3-2
	3.3 B/H/O/C Kinetics	3-4
	3.4 H/O/C Kinetics	3-6
4.0	MODEL RESULTS	4-1
	4.1 B/H/O/C Systems	4-1
	4.2 Isothermal B/H/O/C/F Systems	4-4
	4.3 Adiabatic B/H/O/C/F Systems	4-12
5.0	REACTION FLUX AND SENSITIVITY ANALYSIS	5-1
	5.1 Reaction Flux Analysis	5-1
	5.2 Gradient Sensitivity Analysis	5-11
6.0	SUMMARY	6-1
7.0	REFERENCES	7-1

LIST OF FIGURES

Figure		Page
1.	Equilibrium species mole fractions for F-HMX/TMETN mixture at 1000 psi. . .	2-4
2.	Equilibrium species mole fractions for F-HMX/TMETN/B(s) mixture at 1000 psi. Boron/fluorine and boron/oxygen mole ratios are 0.49 and 0.52, respectively. . .	2-6
3.	Equilibrium species mole fractions for F-HMX/TMETN/B(s) mixture at 1000 psi. Boron/fluorine and boron/oxygen mole ratios are 0.98 and 1.04, respectively. . .	2-7
4.	Equilibrium species mole fractions for F-HMX/TMETN/B(s) mixture at 1000 psi. Boron/fluorine and boron/oxygen mole ratios are 1.96 and 2.07, respectively. . .	2-8
5.	Species and temperature profiles for an adiabatic constant pressure mixture of BO, H_2, CO, O_2 and N_2. Initial conditions: X(BO) = 0.05, $X(H_2)$ = 0.06342, X(CO) = 0.03902, $X(O_2)$ = 0.16586, $X(N_2)$=0.6817, T = 1800 K, P = 1 atm	4-2
6.	Species and temperature profiles for an adiabatic constant pressure mixture of B_2O_2, H_2, CO, O_2 and N_2. Initial conditions: $X(B_2O_2)$ = 0.025, $X(H_2)$ = 0.065, X(CO) = 0.04, $X(O_2)$ = 0.17, $X(N_2)$ = 0.70, T = 1800 K, P = 1 atm.	4-3
7.	Species mole fractions versus time for an isothermal mixture of B(g), F(g), O(g) and N_2(g). Initial conditions: T = 2500 K, P = 1.0 atm, mole fractions X(B) = 0.01, X(F) = 0.01, X(O) = 0.01 and $X(N_2)$ = 0.97.	4-7
8.	Species mole fractions versus time for an isothermal mixture of B(g), F(g), O(g) and N_2(g). Initial conditions: T = 2500 K, P = 1.0 atm, mole fractions X(B) = 0.01, X(F) 0.02, X(O) = 0.005 and $X(N_2)$ = 0.965.	4-8
9.	Species mole fractions versus time for an isothermal mixture of B(g), F(g), O(g) and N_2(g). Initial conditions: T=2500 K, P = 1.0 atm, mole fractions X(B) = 0.01, X(F) = 0.005, X(O) = 0.02 and $X(N_2)$ = 0.965.	4-9

LIST OF FIGURES (Continued)

Figure		Page
10.	Species mole fractions versus time for an isothermal mixture of B(g), F(g), O(g), H(g) and N_2(g). Initial conditions: T = 2500 K, P = 1.0 atm, mole fractions X(B) =0.01, X(F) = 0.02, X(O) = 0.005, X(H) = 0.01 and $X(N_2)$ = 0.955	4-10
11.	Species mole fractions versus time for an isothermal mixture of B(g), F(g), O(g), H(g) and N_2(g). Initial conditions: T=2500 K, P=1.0 atm, mole fractions X(B) = 0.01, X(F) = 0.005, X(O) = 0.02, X(H) = 0.01 and $X(N_2)$ = 0.955	4-11
12.	Species and temperature profiles for an adiabatic, constant pressure system with an initial temperature of 1800K and a pressure of 1 atm. Initial conditions: X(BF) = 0.16, $X(BF_2)$ = 0.11, X(BO) = 0.04, $X(B_2O_2)$ = 0.09, X(OBF) = 0.03, X(CO) = 0.04, $X(H_2)$ = 0.04, $X(O_2)$ = 0.13, $X(H_2O)$ = 0.0, X(HF) = 0.0, $X(N_2)$ = 0.36	4-14
13.	Species and temperature profiles for an adiabatic, constant pressure system an initial temperature of 1800K and a pressure of 1 atm. Initial conditions: X(BF) = 0.16, $X(BF_2)$ = 0.11, X(BO) = 0.04, $X(B_2O_2)$ = 0.09, X(OBF) = 0.03, X(CO) =0.04, $X(H_2)$ = 0.04, $X(O_2)$ = 0.0, $X(H_2O)$ = 0.13, X(HF) = 0.0, $X(N_2)$ = 0.36	4-16
14.	Species and temperature profiles for an adiabatic, constant pressure system with an initial temperature of 1800K and a pressure of 1 atm. Initial conditions: X(BF) = 0.16, $X(BF_2)$ = 0.11, X(BO) = 0.04, $X(B_2O_2)$ = 0.09, X(OBF) = 0.03, X(CO) = 0.04, $X(H_2)$ = 0.04, $X(O_2)$ = 0.0, $X(H_2O)$ = 0.0, X(HF) = 0.13, $X(N_2)$ = 0.36	4-18
15.	Species and temperature profiles for an adiabatic, constant pressure system with an initial temperature of 1800K and a pressure of 1 atm. Initial conditions: X(BF) = 0.16, $X(BF_2)$ = 0.11, X(BO) = 0.04, $X(B_2O_2)$ = 0.09, X(OBF) = 0.03, X(CO) = 0.04, $X(H_2)$ = 0.04, $X(C_2)$ = 0.13, X(H2O) = 0.13, X(HF) = 0.13, $X(N_2)$ = 0.13	4-20

LIST OF FIGURES (Continued)

Figure		Page
16.	Species and temperature profiles for an adiabatic, constant pressure system with an initial temperature of 1800K and a pressure of 1 atm. Initial conditions: X(BF) = 0.16, X(BF_2) = 0.11, X(BO) = 0.04, X(B_2O_2) = 0.09, X(OBF) = 0.03, X(CO) = 0.04, X(H_2) = 0.04, X(O_2) = 0.13, X(H_2O) = 0.07, X(HF) = 0.13, X(N_2) = 0.16	4-22
17.	Reaction flux profiles of OBF. The initial conditions are the same as those of Figure 15	5-3
18.	Reaction flux profiles for BF (part a) and BF_2 (part b). The initial conditions are the same as those of Figure 15	5-4
19.	Reaction flux profiles for HF (part a) and BF_3 (part b). The initial conditions are the same as those of Figure 15	5-5
20.	Reaction flux profiles for BO (part a) and BO_2 (part b). The initial conditions are the same as those of Figure 15	5-6
21.	Reaction flux profiles for B_2O_2 (part a) and B_2O_3 (part b). The initial conditions are the same as those of Figure 15	5-7
22.	Reaction flux profiles for HBO (part a) and HBO_2 (part b). The initial conditions are the same as those of Figure 15	5-8
23.	Reaction flux profiles for O_2 (part a) and H_2O (part b). The initial conditions are the same as those of Figure 15	5-9
24.	Reaction flux profiles for CO (part a) and H_2 (part b). The initial conditions are the same as those of Figure 15	5-10
25.	Sensitivity gradient profiles for OBF. The initial conditions are the same as those of Figure 15	5-13
26.	Sensitivity gradient profiles for BF (part a) and BF_2 (part b). The initial conditions are the same as those of Figure 15	5-14

LIST OF FIGURES (Continued)

Figure		Page
27.	Sensitivity gradient profiles for HF (part a) and BF_3 (part b). The initial conditions are the same as those of Figure 15	5-15
28.	Sensitivity gradient profiles for BO (part a) and BO_2 (part b). The initial conditions are the same as those of Figure 15	5-16
29.	Sensitivity gradient profiles for B_2O_2 (part a) and B_2O_3 (part b). The initial conditions are the same as those of Figure 15	5-17
30.	Sensitivity gradient profiles for HBO (part a) and HBO_2 (part b). The initial conditions are the same as those of Figure 15	5-18
31.	Sensitivity gradient profiles for O_2 (part a) and H_2O (part b). The initial conditions are the same as those of Figure 15	5-19

LIST OF TABLES

Table		Page
1.	Prototypical Fluoroamino/Nitroamino/B(s) System	2-1
2.	Thermochemical Parameters for Dominant Gas Phase Species	2-3
3.	Dominant Boron Speciation in F-HMX/TMETN/B(s) Mixtures	2-9
4.	Reactants for B/H/O/C/F kinetic model	3-1
5.	B/H/O/C/F Reaction Mechanism and Rate Parameters	3-3
6.	B/H/O/C Reaction Mechanism and Rate Parameters	3-5
7.	H/O/C Reaction Mechanism and Rate Parameters	3-6
8.	Initial Conditions for Isothermal Calculations	4-4
9.	Initial Conditions for Adiabatic Calculations	4-12
10.	Dominant Production/Consumption Reactions from Reaction Flux Analysis	5-2
11.	Important Reaction Pathways from Gradient Sensitivity Analysis	5-12

EXECUTIVE SUMMARY

This document is the final report to the Office of Naval Research on work performed under contract N00014-91-C-0141. It presents the results of research preformed by Aerodyne Research, Inc. and Princeton University between June 26, 1991 and June 25, 1992.

This program's research objectives were: (a) to formulate a kinetic model for the homogeneous gas phase chemistry associated with particulate boron oxidation in systems based on fluoroamino/nitroamino oxidizers and (b) to use gradient sensitivity analysis to identify the most important kinetic pathways. The motivation for this work was twofold. The first stemmed from advanced underwater explosive concepts based on mixed nitramine difluoramino explosives, dintroamino salts, energetic polymers and aluminum and boron particles. The second motivation arose from theoretical analyses which suggested that highly energetic, low signature rocket ignition systems might be fashioned from advanced fluorine producing solid oxidizers combined with particulate boron as a fuel. Both applications would benefit from a detailed model for particulate boron combustion in the fluorine rich environments.

The research summarized in this report supports the development of a full particle combustion model by providing a detailed gas phase kinetic mechanism for high temperature B/H/O/C/F mixtures. Specifically, under this program the following research tasks have been accomplished.

1. The scientific literature has been surveyed for available thermochemical parameters and measured reaction rates relevant to high temperature B/H/O/C/F chemistry.

2. Thermodynamic equilibrium calculations have been preformed to provide estimates of the dominant chemical speciation in boron lean and boron rich mixtures. The latter approximates the boundary layer speciation near an individual particle.

3. A kinetic mechanism has been formulated high temperature B/H/O/C/F chemistry. This includes re-evaluation of our earlier B/H/O/C reaction mechanism in light of more recent thermochemical and kinetic data.

4. Detailed kinetic calculations have been preformed to investigate the general mechanistic behavior of fluoroamino/nitroamino/B(s) systems. Emphasis has been given to the affect of changes in the boron/oxygen and boron/fluorine mole ratios.

5. Reaction flux and gradient sensitivity analysis has been used to identify the most important reaction pathways.

The results of this work indicate that fluorine has a significant impact on particulate boron oxidation. Whereas $HBO_2(g)$ and $B_2O_3(g)$ are the dominant oxidation products in B/H/O/C systems,

OBF(g) was consistently found to be the major high temperature combustion product in fluorine enriched environments. Thermodynamic analysis and kinetic calculations suggests that post combustion gases will not contain liquid B_2O_3 for oxygen/fluorine mole ratios near unity. The model results also indicate that the gas phase kinetics is faster and that the energy release is greater when the combustion system is enhanced with fluorine. Lastly, equilibrium results indicate that condensed boron nitride is unlikely to be a dominant combustion product under typical combustion conditions.

Reaction flux and sensitivity analysis have been used to identify important reaction pathways. Based on these results a set of reactions requiring critical experimental/theoretical study have been identified. These reactions include 15 reactions involving boron fluorides and oxyfluorides in addition to a number of B/H/O/C reactions which are important in environments containing oxygen.

Further research is currently being directed towards extending this modeling effort by incorporating heterogeneous reactions.

1.0 INTRODUCTION

Elemental boron has been of interest as an advanced fuel for several decades because of it's high energy density. Recently, there has been an increased interest in particulate boron oxidation in fluorine enriched environments. This interest has arisen, in part, from potential applications of difluoroamino based oxidizers and solid boron in advanced underwater explosive concepts, new propellant formulations and solid propellant ignition systems. The potential advantages of fluorine oxidation include elimination of condensed phase boron oxides and oxyhydrides, as well as faster burn times. Additionally, fluorine has been found to be beneficial in enhancing boron's ignition characteristics by promoting gasification of the oxide layer formed in the presence of oxygen.

Much of the interest in fluorine based oxidizers stems from the large heats of reaction associated boron fluorination. The gravimetric and volumetric heats of formation for BF_3 are 105.01 KJ/g and 245.72 KJ/cc, respectively. Comparison to the heats for formation for B_2O_3, 58.74 KJ/g and 137.45 KJ/cc, illustrates the potential advantage of fluorination. In addition, boron fluorides are gaseous at room temperature and stable at low pressures and high temperatures. In environments containing both oxygen and fluorine, boron combustion may result in stable oxyfluorides.The gravimetric and volumetric heats of reaction to yield OBF, for example, are 55.7 KJ/g and 130.3 KJ/cc, respectively. Thus, oxidation of boron to yield OBF is nearly as energetic as oxidation to solid B_2O_3. The extent to which the thermodynamic potential of boron/fluorine systems is realized, however, ultimately depends on a detailed understanding of the combustion kinetics.

The goal of the present program is to develop a kinetic model for boron combustion that can be used in helping to identify critical parameters and, in conjunction with experimental studies, to better understand combustion mechanisms. Since particulate boron combustion is a complex multistep process involving both heterogeneous and homogeneous chemical kinetics this is an inherently mutiphased task. Consequently, the approach of the current program is to develop a complete combustion model in successive stages. Each stage can be view as a submodel of the complete process and progressively builds on the preceding stages by incorporating additional chemical processes. Thus, the model for combustion of a single boron particles represents a submodel of a full multidimensional particle cloud description of the combustion process. Similarly, kinetic models for homogeneous gas phase and heterogeneous surface oxidation are basic components for the single particle combustion model.

As the first stage in this program, this report summarizes modeling results for the gas phase chemistry associated with particulate boron combustion in fluorine enriched environments. It includes, a description of a reaction mechanism for high temperature B/H/O/C/F combustion systems, the results of kinetic calculations illustrating the mechanistic behavior of these systems, and an analysis of the major reaction fluxes and key reaction pathways. The specific objectives are to characterize the general mechanistic behavior of these systems and to determine the most important gas phase reaction pathways. This provides the basis for identifying those reaction rate parameters whose experimental/theoretical evaluation would significantly enhance the reliability of the model, and hence, our ability to simulate the combustion process in practical applications.

The present model represents an extension of an earlier model for particulate boron oxidation in hydrocarbon combustion environments. In that work, models were developed for both the homogeneous[1-3] and heterogeneous[3-5] kinetics associated with particulate boron in post-hydrocarbon combustion gases. The heterogeneous processes treated included both the high temperature surface burning of a relatively 'clean' boron particle[5] and chemically facilitated gasification of the boron oxide coating[4] that invaribly arises when oxygen is present. In this report, the oxidation model for B/H/O/C combustion systems is extended to include fluorine chemistry.

The kinetic model described in this report is intended for simulations of the gas phase chemistry associated with the oxidation of particulate boron in an environment containing post-combustion products composed of carbon, oxygen, hydrogen and fluorine. Detailed kinetic mechanisms for the fluoroamino/nitroamino solid propellant/explosive combustion are not presented. In addition, nitrogen chemistry has not been included. Reactions involving carbon fluoride and oxyfluoride intermediates have also been neglected since thermodynamic calculations indicated that these species are relatively minor.

The remainder of this report is organized as follows. The equilibrium thermochemistry for a prototypical fluoroamino/nitroamino/B(s) system is discussed in Section 2.0. The reaction mechanism adopted to simulate high temperature, gas phase B/H/O/C/F kinetics is presented in Section 3.0. The results of kinetic calculations for several isothermal and adiabatic, constant pressure systems are described in Section 4.0. Reaction flux and gradient sensitivity analysis results, including identification of the most important reaction pathways, are presented in Section 5.0. General conclusions are summarized in Section 6.0. Technical references are listed in Section 7.0.

2.0 THERMOCHEMISTRY

This section discusses the thermochemistry of fluoroamino/nitroamino based oxidizers with particulate boron fuel. The objectives are: (1) to characterize the equilibrium speciation for a prototypical system and (2) to use the equilibrium results as a quide in selecting the gas phase reactants to be included in the kinetic model.

2.1 Oxidizer/Fuel Mixture Composition

The fluoroamino/nitroamino based oxidizers of current interest include fluorinated derivatives of cyclotetramethylene tetranitramine (HMX) in conjunction with a nitroamino binder. The fluorinated derivatives of HMX result, in part, from the replacement of $-NO_2$ groups by $-NF_2$. As a typical example, the equilibrium calculations summarized below specifically treat the fluorinated HMX derivative (hereafter designated F-HMX) whose empirical formula is given by $C_6H_8N_8O_4F_8$.[6] TMETN ($C_5H_8N_3O_9$) will be used as the binder. The maximum loading of F-HMX in the F-HMX/TMETN mixture is approximately 75% by volume (80:20 by mass).[6] This results in a fixed oxygen/fluorine mole ratio of 0.94. The mass fraction of B(s) is varied to illustrate the equilibrium speciation for a range of boron/fluorine mole ratios. The system's composition and relevant heats of formation are summarized in Table 1.

Table 1. Prototypical Fluoroamino/Nitroamino/B(s) System

Component	Empirical Formula	$\Delta H_{f,\,298}$ (Kcal/mol)	Composition
F-HMX	$C_6H_8N_8O_4F_8$	-45	F-HMX/TMETN ratio fixed at 75% F-HMX by volume
TMETN	$C_5H_8N_3O_9$	-103	"
Boron	B(s)	0	Varied

2.2 Equilibrium Calculations Overview

Constant temperature/pressure equilibrium species mole fractions for various F-HMX/ TMETN/B(s) mixtures were determined to establish initial estimates of the gas phase speciation. The mass fraction of the B(s) component was varied to partially approximate the system's spatial heterogeneity. Boron rich mixtures, for example, were used to characterize the boundary layer speciation near an individual particle. Thus, a series of calculations were performed in which the mass ratio of F-HMX to TMETN was fixed at 400% (75 % by volume) while the mass ratio of the F-HMX/TMETN component to condensed phase B(s) was varied. The latter variations are reported here as changes in the boron/fluorine (B/F) and boron/oxygen (B/O) mole ratios. Calculations were performed for a pressure of 1000 psi and for temperatures ranging between 2000 K and 5000 K.

Thermochemical parameters for the dominant species are summarized in Table 2. The heat of formation for HBO(g) is from Page.[7] The heat of formation for HO_2 is from Hills and Howard[8]. The remaining data is from JANNAF thermochemical tabulations.[9] Uncertainties in thermochemical data for boron species are typically relatively large. For example, uncertainties in heats of formation are on the order of 3 Kcal/mol for BF, BF_2 and OBF and 2 Kcal/mol for BO, BO_2 and B_2O_2. In contrast, typical uncertainties for simple H/O/C compounds are less than 0.1 Kcal/mol. Additionaly, Page's evaluation[7] of the heat of formation for HBO using ab initio MCSCF calculations (-60 Kcal/mol) relative to the JANNAF tabulated value[9] (-47.4 ±3 Kcal/mol) suggests that the uncertainties in thermochemical parameters of boron compounds could be considerably larger than those listed in the JANNAF tabulations.

Table 2. Thermochemical Parameters for Dominant Gas Phase Species

	$\Delta H_{f,298}$	S_{298}	Cp,300	Cp,400	Cp,500	Cp,600	Cp,800	Cp,1000	Cp,1500
H	52.10	27.39	4.97	4.97	4.97	4.97	4.97	4.97	4.97
O	59.55	38.47	5.23	5.14	5.08	5.05	5.02	5.00	4.98
OH	9.32	43.89	7.15	7.10	7.07	7.06	7.13	7.33	7.87
H_2	0.00	31.21	6.90	6.96	7.00	7.02	7.07	7.21	7.73
O_2	0.00	49.00	7.01	7.22	7.44	7.65	8.07	8.35	8.72
H_2O	-57.79	45.11	8.00	8.23	8.44	8.67	9.22	9.87	11.26
HO_2	3.00	54.43	8.36	8.95	9.48	9.96	10.75	11.37	12.34
H_2O_2	-32.53	55.66	10.41	11.44	12.34	13.11	14.29	15.21	16.85
CO	-26.42	47.21	6.95	7.03	7.14	7.27	7.61	7.95	8.41
CO_2	-94.05	51.00	8.91	9.86	10.65	11.31	12.32	12.99	13.93
HCO	10.40	53.66	8.24	8.78	8.28	9.77	10.74	11.52	12.56
B	133.8	36.65	4.97	4.97	4.97	4.97	4.97	4.97	4.97
BO	0.00	48.63	7.00	7.21	7.39	7.57	7.86	8.11	8.53
BO_2	-68.00	54.93	2.54	12.81	13.05	13.27	13.64	13.94	14.43
B_2O_2	-109.00	57.98	15.79	16.32	16.80	17.24	18.00	18.61	19.65
B_2O_3	-199.80	67.80	19.19	19.88	20.52	21.10	22.09	22.90	24.26
HBO	-60.00	48.40	9.38	9.93	10.42	10.88	11.66	12.31	13.42
HBO_2	-134.00	57.30	11.95	12.67	13.34	13.94	15.01	15.89	17.47
F	18.98	37.94	5.25	5.22	5.19	5.16	5.12	5.08	5.02
BF	-27.70	47.923	7.65	7.80	7.93	8.06	8.28	8.46	8.77
BF_2	-137.70	59.07	11.73	11.98	12.21	12.41	12.76	13.03	13.48
BF_3	-271.40	60.74	15.65	16.11	16.54	16.92	17.59	18.12	18.99
OBF	-143.90	53.73	11.69	12.03	12.34	12.63	13.12	13.51	14.18
HF	-65.14	41.53	6.36	6.49	6.62	6.74	6.98	7.20	7.67
N_2	0.0	45.77	6.95	7.01	7.08	7.19	7.50	7.83	8.32

2.3 F-HMX/TMETN Mixture

Equilibrium species mole fractions between 2000 K and 5000 K for a 80:20 (by weight) F-HMX/TMETN mixture at a pressure of 1000 psia are shown in Figure 1. The dominant equilibrium products for this mixture are HF(g), CO(g), and N_2(g). Additionally, H_2(g) is present at a mole fraction ranging between 0.05 and 0.08. The mole fractions for these diatomics tend to decrease at highter temperatures. For example, there is a notable decrease in the mole fraction of HF(g) for temperatures greater than ca. 4000 K. Similarly, the mole fraction of H_2(g) decreases monotonically over the entire temperature range. The high temperature falloff in HF(g) and H_2(g) is accompanied by corresponding increases in the equilibrium levels of atomic hydrogen and fluorine.

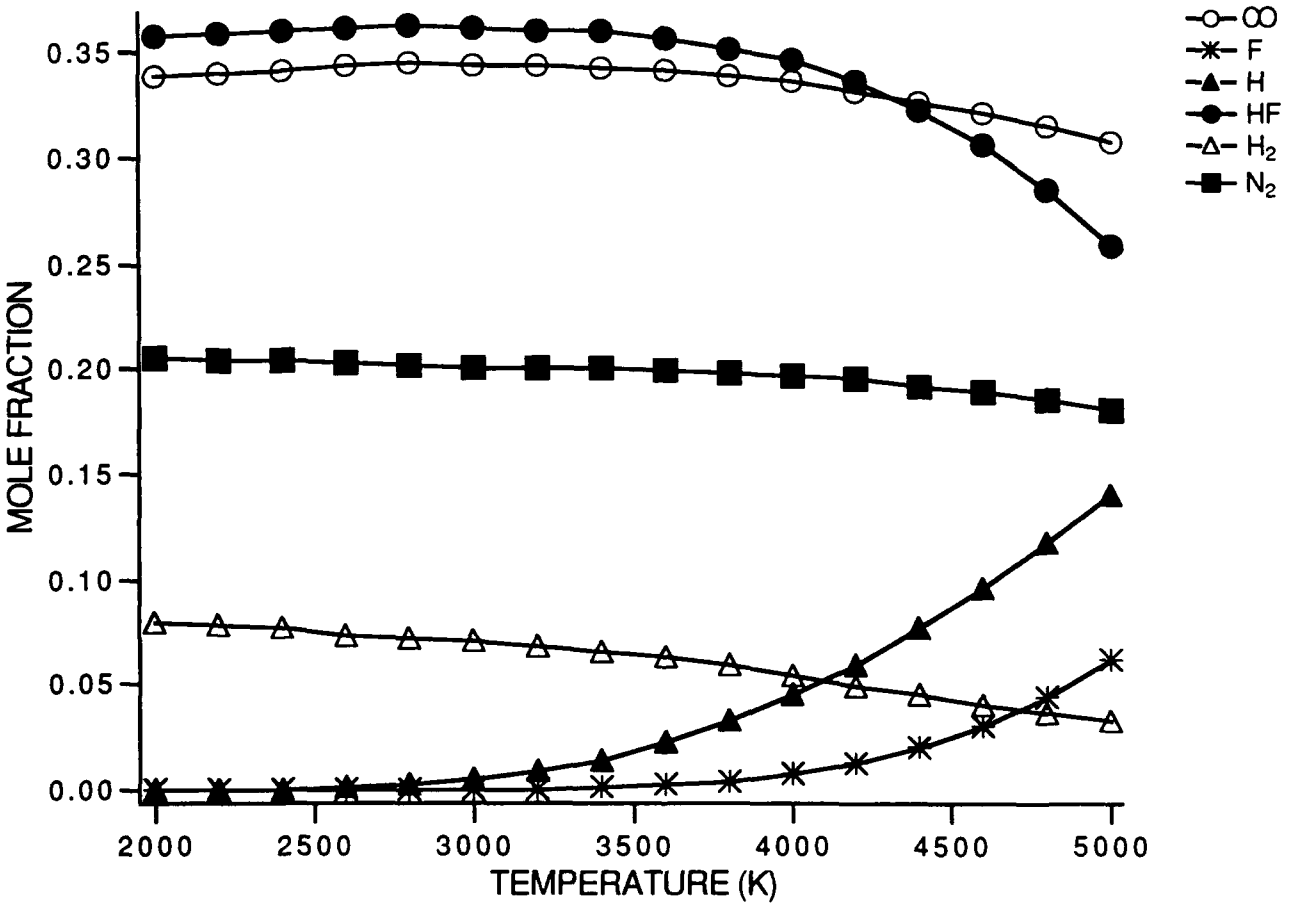

Figure 1. Equilibrium species mole fractions for F-HMX/TMETN mixture at 1000 psi.

2.4 F-HMX/TMETN/B(s) Mixtures

Equilibrium species mole fractions versus temperature for a relatively boron lean mixture are displayed in Figure 2. The mass ratio of F-HMX/TMETN to B(s) for this case corresponds to B/F and B/O mole ratios of 0.49 and 0.52, respectively.

Compared to Figure 1, it can be seen that there is a strong redistribution of fluorine when boron is present in the mixture. Specifically, the HF(g) mole fraction is significantly reduced over the entire temperature range and is particularly low for temperatures between 2000 K and ca. 2700 K. For the latter temperature range, BF_3(g) is the dominant fluorine containing species. At temperatures above 2600 K, BF_2(g) and BF(g) replace BF_3(g) as the florine containing species with the largest mole fractions, with BF(g) dominating at temperatures above ca. 3800 K. The OBF(g) mole fraction is non-negligible, but less than the mole fractions of HF(g) or boron fluorides over the entire temperature range.

Similar trends are seen in Figure 3. In this case the mass ratio of F-HMX/TMETN to B(s) was choosen to correpsond to B/F and B/O mole ratios of 0.98 and 1.04 . The BN(s) phase is shown to persist upto ca. 3200 K while BF_3 and BF_2 are the gas phase fluorine containing species with the largest mole fraction. Again, BF_3(g) is dominant for temperatures between 2000 K and 2600 K, while the mole fraction of BF_2(g) and BF(g)) increase as the temperature increases.

Equilibrium species mole fraction temperature profiles for a boron rich F-HMX/ TMETN/B(s) mixture are displayed in Figure 4. B/F and B/O mole ratios for this case are 1.96 and 2.07, respectively. Here it can be seen that the equilibrium mixture is dominated by condensed phases of BN(s) and B(l) for temperatures upto ca. 3500 K. Particularly interesting is the evolution of boron speciation with increasing temperature. Up to ca. 2700 K, most of the boron is in the form of BN(s). Between 3100 K and 4500 K, the BN(s) phase is replaced by B(l) and N_2(g) with lesser amounts of BF(g) and BF_2(g). The latter two species are the dominant gas phase boron species for 2500 K < T < 5000 K, while OBF(g) is the primary gas phase boron containg species fot 2000 K < T < 2500 K.

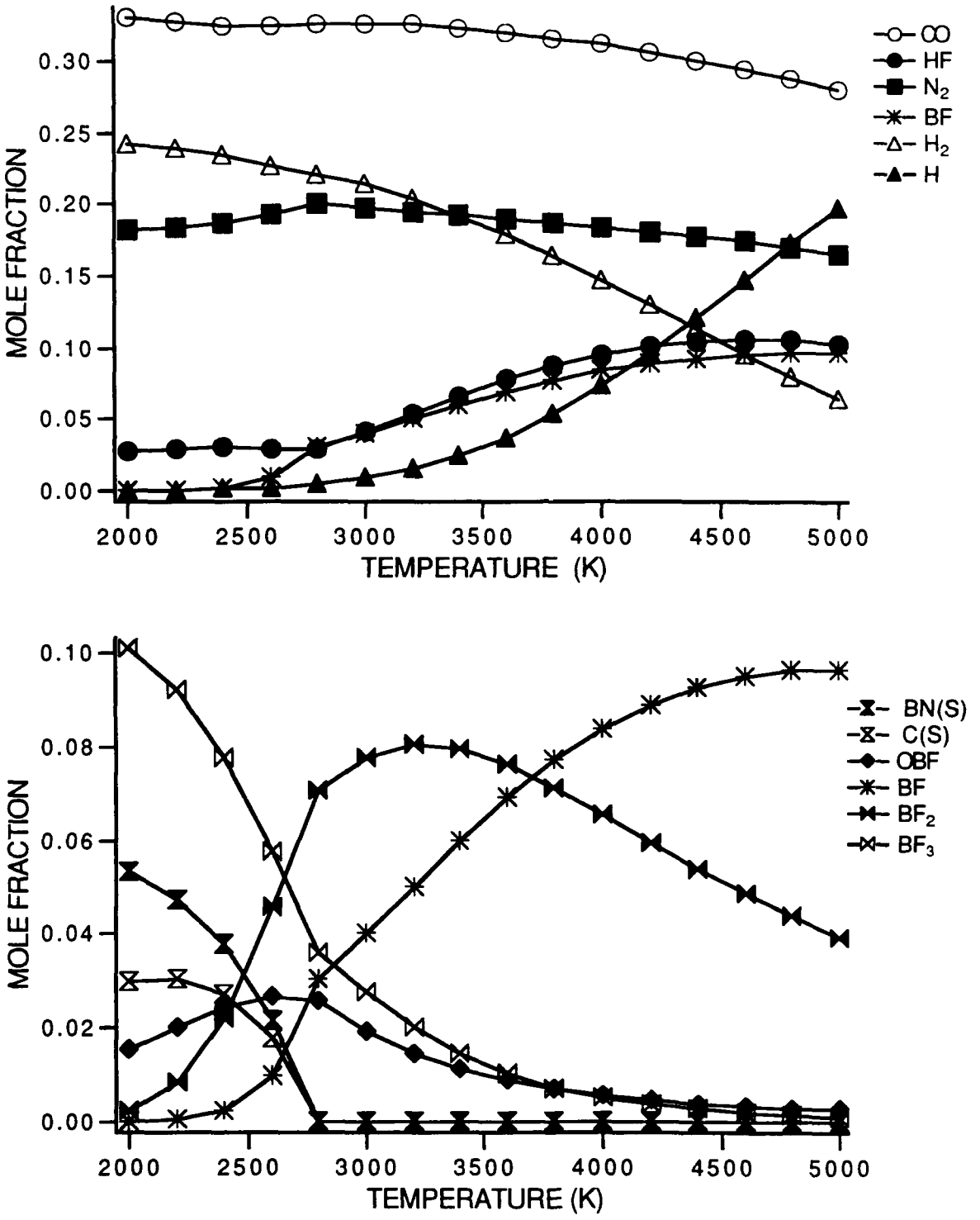

Figure 2. Equilibrium species mole fractions for F-HMX/TMETN/B(s) mixture at 1000 psi. Boron/fluorine and boron/oxygen mole ratios are 0.49 and 0.52, respectively.

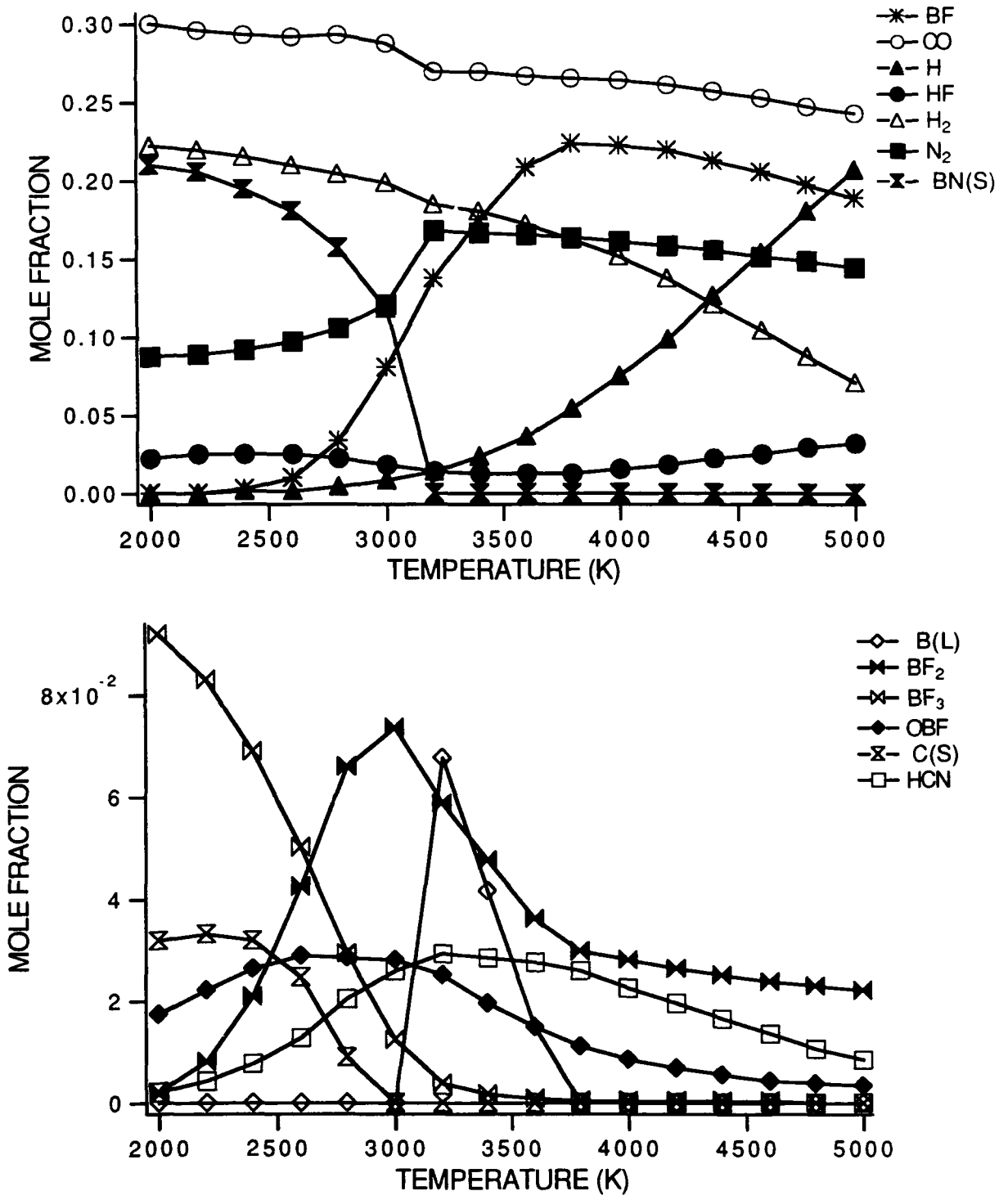

Figure 3. Equilibrium species mole fractions for F-HMX/TMETN/B(s) mixture at 1000 psi. Boron/fluorine and boron/oxygen mole ratios are 0.98 and 1.04, respectively.

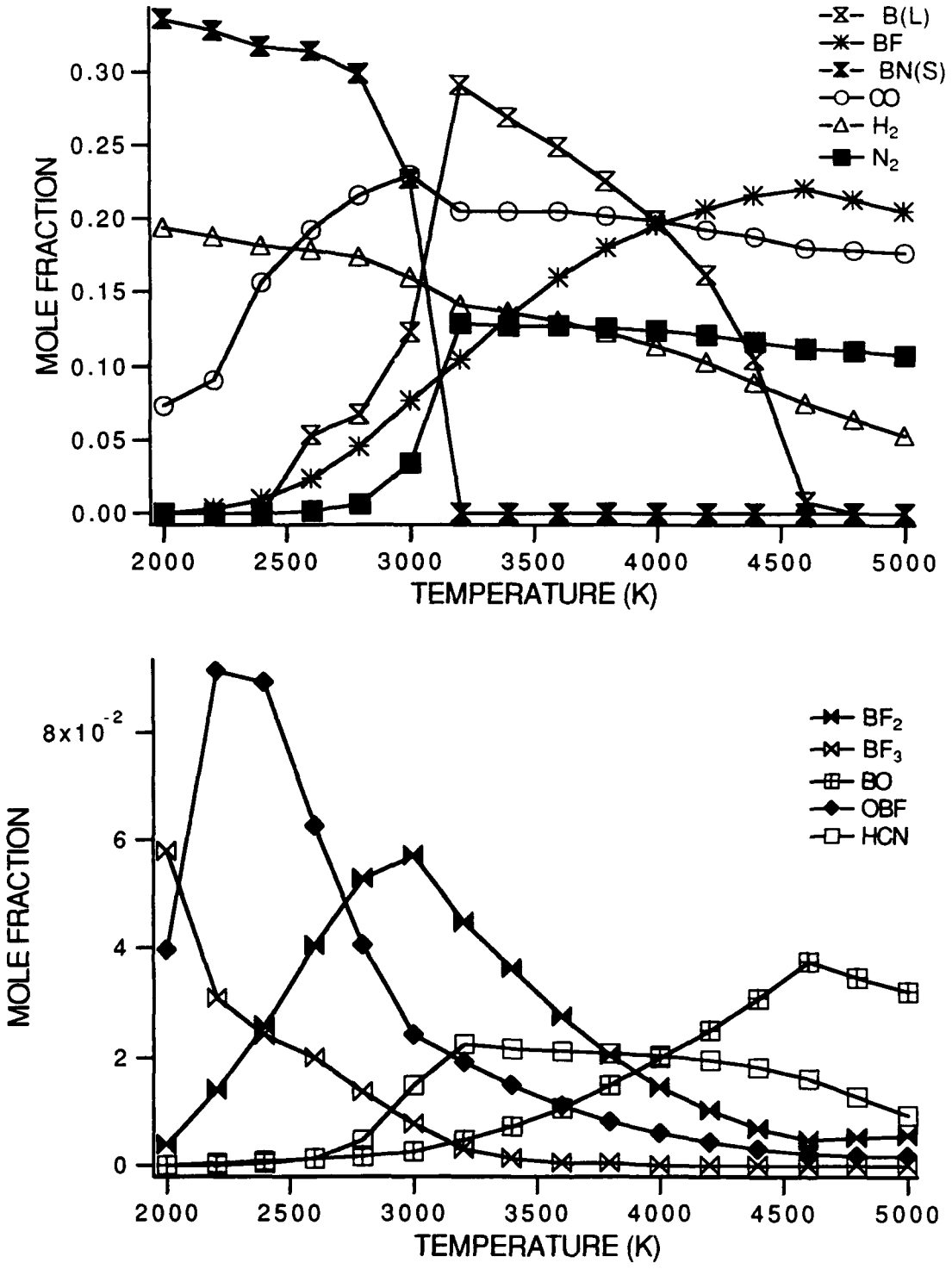

Figure 4. Equilibrium species mole fractions for F-HMX/TMETN/B(s) mixture at 1000 psi. Boron/fluorine and boron/oxygen mole ratios are 1.96 and 2.07, respectively.

Based on these results, the dominant boron speciation in F-HMX/TMETN/B(s) mixtures has been summarized in Table 3 at four temperature for each of the three mixtures described above. For each mixture and temperature, species are listed in order of decreasing mole fraction. Species whose mole fraction is less than 0.01 are not included.

Table 3. Dominant Boron Speciation in F-HMX/TMETN/B(s) Mixtures

B/F and B/O mole fraction	2000 K	3000 K	4000 K	5000 K
B/F = 0.49 B/O=0.52	BF_3 BN(S) HF OBF	BF_2 HF BF BF_3 OBF	HF BF BF_2 OBF BF_3	HF BF BF_2
B/F = 0.98 B/O = 1.04	BN(S) BF_3 OBF	BF_2 BF OBF HF BF_3	BF BF_2 OBF	HF BF BF_2 OBF
B/F = 1.96 B/O = 2.07	BN(S) BF_3 OBF BF_2	BF_2 BF OBF BF_3	BF BO BF_2 OBF	BF BO BF_2

It is clear from Table 3, that for a F/O mole ratio near unity, boron fluorides are the dominant boron containing species. BO(g) is the only boron oxide to reach a level comparable to the fluorides, and it has a significant mole fraction only under boron rich conditions and, even then, only at high temperatures.

In addition to the primary speciation displayed in Figure 4, the equilibrium mixture is composed of a host of carbon and nitrogen fluorides/oxyfluorides and. However, the equilibrium mole fractions for these species are less than 10^{-3} and are therefore not shown.

3.0 REACTION MECHANISM

3.1 Gas Phase Reactants

Gas phase reactants were selected for inclusion in the kinetic model based on the equilibrium results presented in Section 2, The selected reactants, as well as their heats of formation and entropies are listed in Table 4. The heat of formation for HBO(g) is based on the theoretical calculations of Page.[7] All other data is from recent JANAF thermochemical tabulations.[9]

Table 4 - Reactants for Gas Phase B/H/O/C/F Kinetic Model

Species	$\Delta H_{f,298}$ (Kcal/mol)		S_{298} (cal/mol-K)	
B(g)	133.8	± 3.	36.65	
BO(g)	0.0	± 0.0	48.63	± 0.01
BO_2(g)	-68.0	± 2.	54.93	± 0.05
B_2O_2(g)	-109.0	± 2.	57.98	
B_2O_3(g)	-199.8	± 1.	67.80	± 1.
HBO(g)	-60.0	± 2.	48.40	± 0.1
HOBO(g)	-134.0	± 0.3	57.20	
BF(g)	-27.7	± 3.3	47.92	
BF_2(g)	-141.0	± 3.1	59.07	± 0.5
BF_3(g)	-271.4	± 0.41	60.74	± 0.01
OBF(g)	-143.9	± 3.1	53.73	
F(g)	18.9	± 0.072	37.94	± 0.001
HF(g)	-65.1	± 0.19	41.53	± 0.008
O(g)	59.6	± 0.024	38.47	± 0.005
H(g)	52.1	± 0.001	27.39	± 0.004
OH(g)	9.3	± 0.24	43.89	± 0.01
O_2(g)	0.0		49.01	± 0.008
H_2(g)	0.0		31.21	± 0.008
H_2O(g)	-57.8	± 0.040	45.11	± 0.01
CO(g)	-26.4	± 0.011	42.21	± 0.01
CO_2(g)	-94.0	± 0.011	51.07	± 0.03
HCO(g)	10.4		53.66	

These species were selected primarily on the basis of the equilibrium results presented in Section 2 and include boron fluorides, oxyfluorides, oxides and oxyhydrides which may result from surface or gas phase oxidation reactions. The reactant list also includes eleven species (F, HF, O, H, OH, O_2, H_2, H_2O, CO, CO_2, HCO) which, to varying degrees, comprise post hydrocarbon or fluoramino combustion environments. Carbon, oxygen and nitrogen fluorides, as well as hydrocarbons are not included since they were found to be relatively minor constituents in both boron rich and boron lean equilibrium mixtures. Boron hydrides are excluded for the same reason. Atomic B(g) has been included, however, even though thermodynamically it is highly unlikely to be an important constituent of these mixtures. The reason is that it's mole fraction is a useful adjustable input parameter in preliminary kinetic calculations to evaluate the effect of changes in the boron/fluorine and boron/oxygen mole ratios.

3.2 B/H/O/C/F Kinetics

Reactions between fluorinated species in Table 4 and boron oxides, boron oxyhydrides and hydrocarbon combustion products are listed in Table 5. Tabulated reaction enthalpies were computed from reactant/product heats of formation using the data in Table 4. The reaction mechanism in Table 5 is limited to bimolecular and ter-molecular third-body reactions. Higher order reactions such as A + B + C = D + E were neglected since they were typically estimated to proceed much slower than the bimolecular reactions listed. For a given set of reactants all product channels resulting in gas phase products consistent with the reactants listed in Table 4 were included. Channels resulting in products not listed in Table 4, e.g. boron hydrides, were excluded to ensure that the mechanism is self-consistent.

Reaction rates for most of the reactions in Table 5 are not known. A literature survey indicated that measured rate parameters for boron fluorides and oxyfluorides have been reported only for reactions between BF and oxidants such as O_2, O and NO_2.[10,11] Consequently, rate parameters had to be estimated. For most of these reactions initial estimates were adopted from the advance propellant afterburning study of Kolb, et.al.[12] Rate parameters for the remaining reactions were obtained using simple scaling relationships based on the ratios of translational, rotational and vibrational partition functions.

Table 5 - B/H/O/C/F Gas Phase Reaction Mechanism and Rate Parameters: $k = A \times T^n \times \exp(E_a/RT)$

	Reaction	ΔH (Kcal/mol)	A* (cc/mol-s)	n	E_a (Kcal/mol)
1.	$B + F + M = BF + M$	- 7.83	$5.00 \times 10^{+15}$	0.0	-1.987
2.	$BO + F + M = OBF + M$	- 7.06	$3.63 \times 10^{+14}$	0.0	-1.987
3.	$BF + O + M = OBF + M$	- 7.62	$3.63 \times 10^{+14}$	-0.5	0.300
4.	$F + H + M = HF + M$	- 5.91	$2.21 \times 10^{+22}$	-2.0	0.0
5.	$BF + F + M = BF_2 + M$	- 5.59	$3.63 \times 10^{+14}$	-0.5	5.961
6.	$BO_2 + F = OBF + O$	- 1.53	$1.20 \times 10^{+14}$	0.0	0.0
7.	$B_2O_2 + F = OBF + BO$	- 2.34	$2.41 \times 10^{+14}$	0.0	0.0
8.	$B_2O_3 + F = OBF + BO_2$	- 1.35	$2.41 \times 10^{+14}$	0.0	0.0
9.	$HBO + F = OBF + H$	- 2.20	$1.08 \times 10^{+14}$	0.0	0.0
10.	$HBO + F = HF + BO$	- 1.05	$3.61 \times 10^{+13}$	0.0	0.0
11.	$HOBO + F = HF + BO_2$	- 0.79	$3.61 \times 10^{+13}$	0.0	0.994
12.	$HOBO + F = OBF + OH$	- 0.85	$1.08 \times 10^{+14}$	0.0	0.0
13.	$B + HF = H + BF$	- 1.92	$3.61 \times 10^{+14}$	0.0	0.0
14.	$BO + HF = OBF + H$	- 1.16	$1.81 \times 10^{+12}$	0.0	6.955
15.	$BO_2 + HF = OBF + OH$	- 0.06	$1.81 \times 10^{+11}$	0.0	9.935
16.	$B_2O_2 + HF = OBF + HBO$	- 1.29	$3.13 \times 10^{+09}$	0.0	9.935
17.	$B_2O_3 + HF = OBF + HOBO$	- 0.56	$6.02 \times 10^{+08}$	0.	11.922
18.	$HBO + HF = OBF + H_2$	- 0.81	$1.81 \times 10^{+11}$	0.0	9.935
19.	$HOBO + HF = OBF + H_2O$	- 0.11	$1.57 \times 10^{+10}$	0.0	9.935
20.	$BO_2 + BF = OBF + BO$	- 2.09	$3.01 \times 10^{+13}$	0.0	1.987
21.	$BO + BF_2 = OBF + BF$	- 1.47	$6.02 \times 10^{+12}$	0.0	0.0
22.	$BO_2 + BF_2 = OBF + OBF$	- 3.56	$1.81 \times 10^{+11}$	0.0	9.935
24.	$BF + O = BO + F$	- 0.56	$8.43 \times 10^{+13}$	0.0	0.0
23.	$B + OBF = BO + BF$	-17.60	$4.22 \times 10^{+10}$	0.0	0.0
25.	$BF_2 + O = OBF + F$	- 2.03	$1.20 \times 10^{+14}$	0.0	0.0
26.	$BF_2 + H = BF + HF$	- 0.31	$3.01 \times 10^{+13}$	0.0	0.0
27.	$F + OH = HF + O$	- 1.47	$3.01 \times 10^{+13}$	0.0	0.397
28.	$BF + OH = OBF + H$	- 3.18	$1.20 \times 10^{+13}$	0.0	0.0
29.	$BF + OH = BO + HF$	- 2.03	$6.02 \times 10^{+11}$	0.0	4.968
30.	$BF_2 + OH = OBF + HF$	- 3.50	$1.81 \times 10^{+12}$	0.0	4.968
31.	$BF + O_2 = OBF + O$	- 2.46	$1.08 \times 10^{+13}$	0.0	14.390
32.	$F + H_2 = HF + H$	- 1.39	$1.63 \times 10^{+14}$	0.0	1.590
33.	$F + H_2O = OH + HF$	- 0.74	$6.02 \times 10^{+13}$	0.0	1.987
34.	$BF_2 + B = BF + BF$	- 2.23	$3.61 \times 10^{+13}$	0.0	0.0
35.	$BF_2 + HF = BF_3 + H$	- 0.71	$1.81 \times 10^{+12}$	0.0	9.935
36.	$BF_3 + B = BF_2 + BF$	- 1.21	$3.61 \times 10^{+13}$	0.0	0.0
37.	$BF_2 + BF_2 = BF_3 + BF$	- 1.03	$6.02 \times 10^{+11}$	0.0	0.0
38.	$BF_3 + BO = BF_2 + OBF$	- 0.44	$6.02 \times 10^{+12}$	0.0	1.987

* For third body reactions A has units of cm^6/mol^2-s

3.3 B/H/O/C Kinetics

Gas phase reactions and rate parameters describing boron chemistry in post hydrocarbon combustion environments are listed in Table 6. This reaction set is an upgraded version of an earlier kinetic model for the gas phase chemistry associated with particulate boron combustion in air-breathing propulsion systems. The current version incorporates recent experimental rate measurements, as well results from theoretical ab initio calculations and gas phase kinetic modeling work.

Experimental rate data for the reactions in Table 6 is very limited. To date, relevant laboratory studies of gas phase reactions have been limited to atomic B and BO with simple stable oxidants such O_2, CO_2 and H_2O. Rate constants for reactions between boron atom and O_2, CO_2 and H_2O have been measured by DiGiuseppe, et. al.[13,14] Room temperature rate measurements for BO + O_2 have been conducted by Llewellyn, et. al.[15] and Oldenberg, et. al.[16,17] The latter observed a slight negative temperature dependence which was attributed to a stable BO_3 intermediate. The rate for this reaction in the temperature range 300-900 K was measured by Stanton et. al.[18] This work confirmed a small (- 0.51 Kcal/mol) negative temperature dependence. The hydrogen abstraction reaction BO + H_2 --> HBO + H has been studied theoretically Page[7] and experimentally by Garland, et. al.[19]

There are some notable differences between the reaction mechanism presented in Table 6 and the model used by Pasternak.[20] As noted above, the present model does not include reactions involving boron hydrides. In addition, because we are primarily interested in the gas phase chemistry between boron containing species evolving from the surface of a boron particle and the post fluoroamino combustion gases, reactions involving gas phase intermediates such as HCO have also been neglected. Lastly, a set of reactions considered by Pasternak[20] are not included in the present model based on kinetic arguments. These reactions are insertion reactions of the general form

H-BO + O-Y ---> HOBO + Y (O-Y = O_2, H_2O, BO, OH, CO_2)

and

OB-BO + O-Y ---> OB-O-BO + Y (O-Y = O_2, H_2O, BO, OH, CO_2).

Although, because of boron's strong electron deficiency, these reactions cannot be definitely ruled out, it would be very surprising if they proceeded at rates which where competitive with alternate reaction channels. They are consequently excluded here until theoretical or experimental data becomes available.

Table 6 - B/H/O/C Gas Phase Reaction Mechanism and Rate Parameters: $k = A \times T^n \times \exp(-E_a/RT)$

Reaction	ΔH_r (Kcal/mol)	A* (cc/mol-s)	n	E_a (Kcal/mol)
39. $B + O_2 = BO + OH$	-74.25	$7.2 \times 10^{+13}$	0.0	0.31
40. $B + O + M = BO + M$	-193.35	$1.1 \times 10^{+15}$	-0.5	-1.99
41. $BO + O_2 = BO_2 + O$	-8.45	$4.2 \times 10^{+12}$	0.0	-0.51
42. $BO + O + M = BO_2 + M$	-127.55	$1.1 \times 10^{+15}$	0.0	-1.99
43. $B + BO_2 = BO + BO$	-65.80	$3.6 \times 10^{+13}$	0.0	0.0
44. $BO + BO_2 + M = B_2O_3 + M$	-131.80	$1.8 \times 10^{+13}$	0.0	-1.99
45. $BO_2 + BO_2 = B_2O_3 + O$	-4.25	$6.0 \times 10^{+10}$	0.0	9.94
46. $B + OH = BO + H$	-91.02	$6.0 \times 10^{+13}$	0.0	0.0
47. $BO + OH = BO_2 + H$	-25.22	$2.4 \times 10^{+12}$	0.0	0.0
48. $BO + OH + M = HOBO + M$	-143.32	$3.6 \times 10^{+14}$	0.0	-1.99
49. $BO + H_2O = HOBO + H$	-24.10	$6.0 \times 10^{+10}$	0.0	-9.94
50. $BO_2 + OH = HOBO + O$	-15.76	$1.8 \times 10^{+12}$	0.0	0.99
51. $BO_2 + H + M = HOBO + M$	-118.10	$1.8 \times 10^{+15}$	0.0	-1.99
52. $BO_2 + H_2 = HOBO + H$	-13.90	$1.8 \times 10^{+12}$	0.0	1.99
53. $HOBO + OH = BO_2 + H_2O$	-1.11	$1.2 \times 10^{+12}$	0.0	1.99
54. $B_2O_3 + H_2O = HOBO + HOBO$	-10.41	$6.0 \times 10^{+08}$	0.0	11.92
55. $BO + H + M = HBO + M$	-112.10	$1.1 \times 10^{+15}$	0.0	-1.99
56. $BO + H_2 = HBO + H$	7.89	$4.5 \times 10^{+01}$	3.53	3.16
57. $BO + OH = HBO + O$	9.76	$1.6 \times 10^{+03}$	2.76	5.01
58. $HBO + O = BO_2 + H$	-15.45	$4.8 \times 10^{+13}$	0.0	5.01
59. $HBO + OH = BO + H_2O$	-7.11	$4.8 \times 10^{+13}$	0.0	0.0
60. $HBO + OH = HOBO + H$	-31.22	$4.8 \times 10^{+13}$	0.0	0.0
61. $HBO + OH = BO_2 + H_2$	-17.32	$6.0 \times 10^{+03}$	0.0	69.94
62. $HBO + O_2 = BO_2 + OH$	1.32	$6.0 \times 10^{+03}$	0.0	69.94
63. $HBO + O + M = HOBO + M$	-133.10	$3.6 \times 10^{+20}$	0.0	50.07
64. $BO + BO + M = B_2O_2 + M$	-109.00	$3.6 \times 10^{+13}$	0.0	-1.99
65. $B_2O_2 + H = HBO + BO$	-3.10	$6.0 \times 10^{+13}$	0.0	0.0
66. $B_2O_2 + O = BO + BO_2$	-18.55	$3.6 \times 10^{+13}$	0.0	0.0
67. $B_2O_2 + OH = BO + HOBO$	-34.32	$3.6 \times 10^{+03}$	0.0	0.0.
68. $B_2O_2 + OH = BO_2 + HBO$	-28.32	$6.0 \times 10^{+03}$	0.0	69.94
69. $B_2O_2 + O_2 = BO_2 + BO_2$	-27.00	$6.0 \times 10^{+03}$	0.0	80.08
70. $BO_2 + CO = BO + CO_2$	0.37	$3.0 \times 10^{+13}$	0.0	1.99
71. $B + H_2O = HBO + H$	-83.90	$2.4 \times 10^{+14}$	0.0	2.68
72. $B + CO_2 = BO + CO$	-66.17	$4.2 \times 10^{+10}$	0.0	0.0
73. $HBO + BO_2 = HOBO + BO$	-6.00	$1.8 \times 10^{+12}$	0.0	0.99
74. $HBO + BO_2 = B_2O_3 + H$	-62.50	$1.8 \times 10^{+12}$	0.0	0.99
75. $HOBO + BO = B_2O_3 + H$	-56.50	$4.8 \times 10^{+12}$	0.0	0.0

* For third body reactions A has units of cm^6/mol^2-s

3.4 H/O/C Kinetics

In addition to the reactions in Tables 5 and 6, the reaction mechanism listed in Table 7 has been included in kinetic calculations to describe the post hydrocarbon combustion involving H/O/C species.[21] This mechanism was originally developed to describe the kinetics of $CO/H_2/O_2$ mixtures.

Table 7 - H/O/C Gas Phase Reaction Mechanism and Rate Parameters: $k = A \times T^n \times \exp(-E_a/RT)$

Reaction	A* (cc/mol-s)	n	E_a (Kcal/mol)
76. $H + O_2 = O + OH$	$1.92 \times 10^{+14}$	0.0	16.440
77. $O + H_2 = H + OH$	$5.08 \times 10^{+04}$	2.7	6.292
78. $OH + H_2 = H + H_2O$	$2.16 \times 10^{+08}$	1.5	3.430
79. $OH + OH = O + H_2O$	$1.23 \times 10^{+04}$	2.6	1.878
80. $H_2 + M = H + H + M$	$4.57 \times 10^{+19}$	1.4	104.4
81. $O + O + M = O_2 + M$	$6.17 \times 10^{+15}$	-0.5	0.0
82. $O + H + M = OH + M$	$4.72 \times 10^{+18}$	-1.0	0.0
84. $H + O_2 + M = HO_2 + M$	$6.63 \times 10^{+13}$	-1.4	0.0
85. $HO_2 + H = H_2 + O_2$	$6.17 \times 10^{+19}$	0.0	2.216
86. $HO_2 + H = OH + OH$	$1.69 \times 10^{+14}$	0.0	0.874
87. $HO_2 + O = OH + O_2$	$8.10 \times 10^{+13}$	0.0	0.397
88. $HO_2 + OH = H_2O + O_2$	$1.45 \times 10^{+16}$	-1.0	0.0
89. $HO_2 + HO_2 = H_2O_2 + O_2$	$3.02 \times 10^{+12}$	0.0	1.390
90. $H_2O_2 + M = OH + OH + M$	$1.20 \times 10^{+17}$	0.0	45.5
91. $H_2O_2 + H = H_2O + OH$	$1.00 \times 10^{+13}$	0.0	3.590
92. $H_2O_2 + H = H_2 + HO_2$	$4.82 \times 10^{+13}$	0.0	7.948
93. $H_2O_2 + O = OH + HO_2$	$9.55 \times 10^{+06}$	2.0	3.970
94. $H_2O_2 + OH = H_2O + HO_2$	$7.00 \times 10^{+12}$	0.0	1.430
95. $CO + O + M = CO_2 + M$	$2.51 \times 10^{+13}$	0.0	4.541
96. $CO + O_2 = CO_2 + O$	$2.53 \times 10^{+12}$	0.0	47.690
97. $CO + OH = CO_2 + H$	$1.50 \times 10^{+07}$	1.3	0.765
98. $CO + HO_2 = CO_2 + OH$	$6.02 \times 10^{+13}$	0.0	22.950
99. $HCO + M = H + CO + M$	$1.86 \times 10^{+17}$	-1.0	17.000
100. $HCO + O_2 = CO + HO_2$	$7.58 \times 10^{+12}$	0.0	0.410
101. $HCO + H = CO + H_2$	$7.23 \times 10^{+13}$	0.0	0.0
102. $HCO + O = CO + OH$	$3.02 \times 10^{+13}$	0.0	0.0
103. $HCO + OH = CO + H_2O$	$3.02 \times 10^{+13}$	0.0	0.0

* For third body reactions A has units of cm^6/mol^2-s

4.0 MODEL RESULTS

The high temperature chemistry described by the reaction mechanism presented in Section 3 was characterized by following the time evolution of several homogenous systems. Both isothermal and adiabatic, constant pressure systems were studied. Initial conditions were varied to examine the response of species mole fraction and temperature profiles. The kinetic equations were solved using CHEMKIN[22], SENKIN[23], DASAC[24], AIM[25], and LSODE[26]. Constant pressure specific heats, enthalpies and entropies for each species were obtained from polynomial fits to the JANNAF thermochemical data.[9]

4.1 B/H/O/C Systems

Before examing the effects of fluorine on boron oxidation kinetics, it is useful to briefly review the kinetic behavior of B/H/O/C systems in light of the more recent experimental and theoretical data discussed in Section 3.3. A more extensive analysis has been reported by Pasternak.[20]

In Figures 5 and 6, kinetic profiles are presented for two systems studied previously.[2] These figures illustrate the kinetics of BO and B_2O_2, respectively, as initial boron suboxides reacting in a bath of H_2, CO, O_2 and N_2. The reaction sequence and rates of reaction are nearly the same as those predicted by the original mechanism[2] with two exceptions. First, the B/H/O/C reaction mechanism in Table 7 predicts a larger concentration of HBO as an intermediate relative to our earlier results. This change was expected based on Page's[7] reported heat of formation for HBO which altered the direction of exothermicity for several HBO reactions. Second, B_2O_3 formation is initiated earlier in the reaction sequence as a result of the reactions

$$HBO + BO_2 = B_2O_3 + H$$

$$HBO_2 + BO = B_2O_3 + H.$$

These differences are consistent with the modeling results reported by Pasternak.[20]

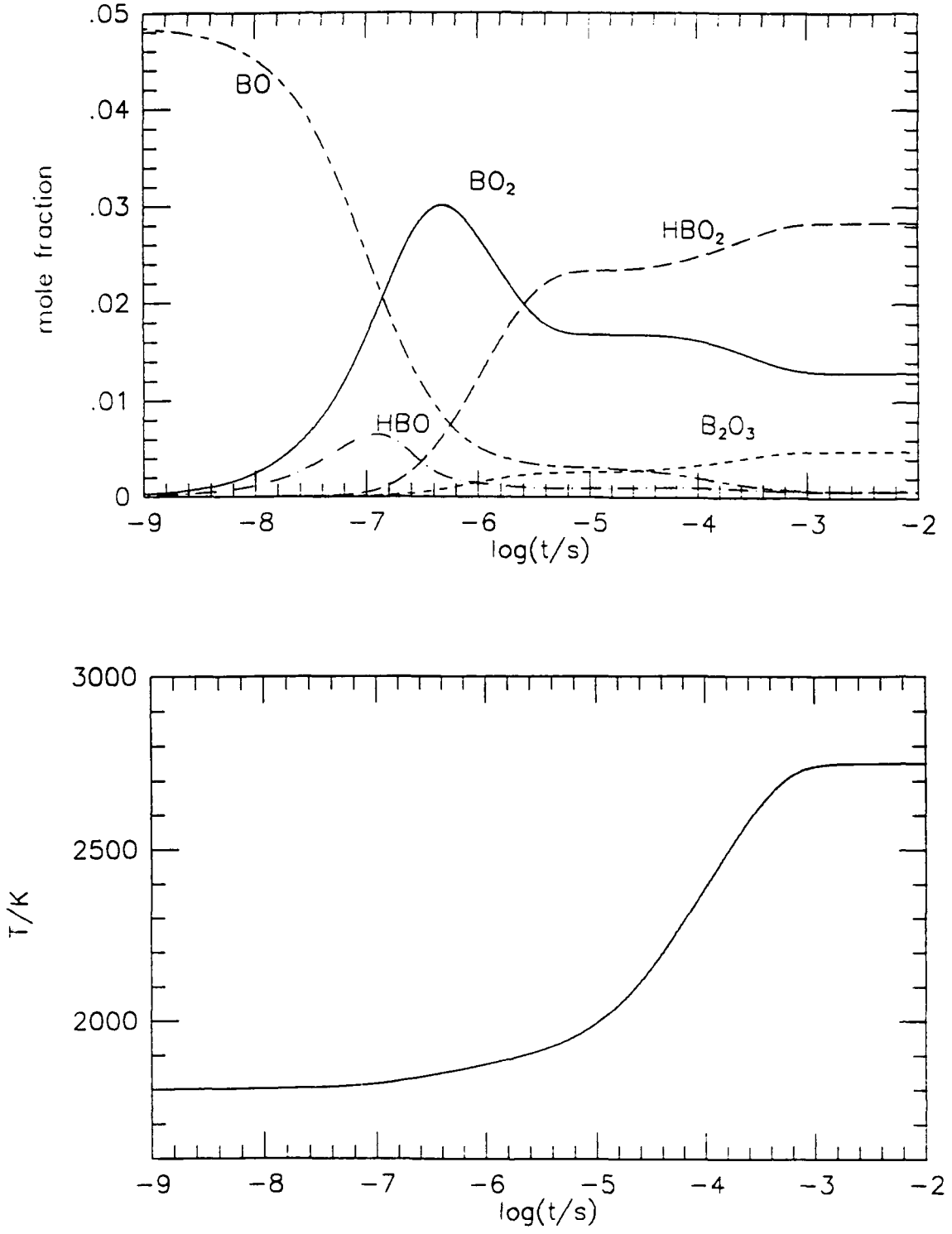

Figure 5. Species and temperature profiles for an adiabatic constant pressure mixture of BO, H_2, CO, O_2 and N_2. Initial conditions: X(BO) = 0.05, X(H_2) = 0.06342, X(CO) = 0.03902, X(O_2) = 0.16586, X(N_2)=0.6817, T = 1800 K, P = 1 atm.

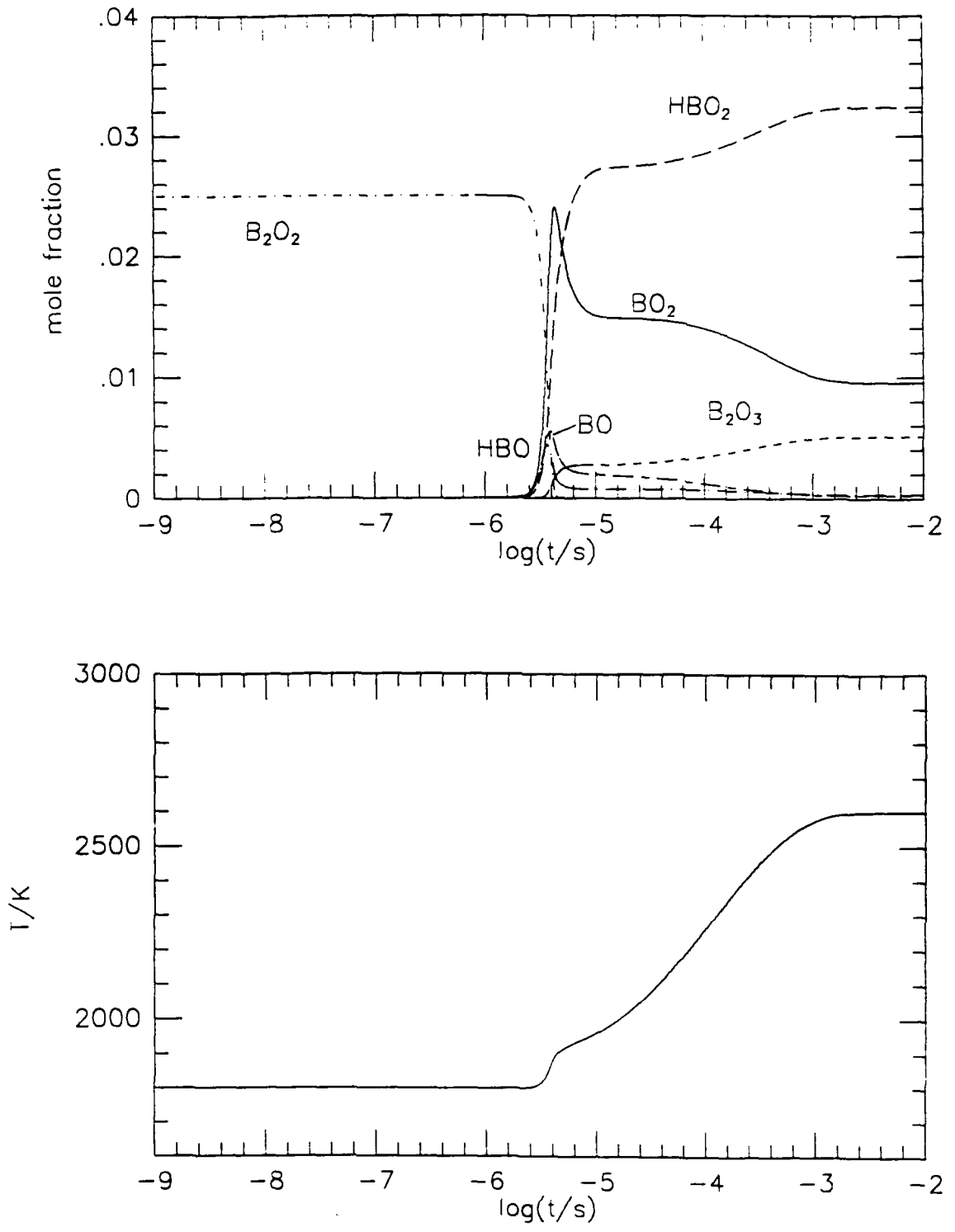

Figure 6. Species and temperature profiles for an adiabatiic constant pressure mixture of B_2O_2, H_2, CO, O_2 and N_2.Initial conditions: $X(B_2O_2) = 0.025$, $X(H_2) = 0.065$, $X(CO) = 0.04$, $X(O_2) = 0.17$, $X(N_2) = 0.70$, T = 1800 K, P = 1 atm.

4.2 Isothermal B/H/O/C/F Systems

A series of isothermal kinetic calculations were performed to evaluate the effect of changes in the O/B, F/B and H/B mole ratios on the gas phase kinetics. Initial conditions for 5 separate calculations are summarized in Table 8. The temperature and pressure for each calculation were 2500 K and 1 atm, respectively. The O/F, F/B and H/B mole ratios were varied by changing initial mole fractions of the reactants which were introduced as atomic species B, O, F and H. Because of boron's low vapor pressure, the results at early reaction times are not relevant to boron particle combustion. However, once all of the gas phase atomic boron has been consumed (ca. 0.001 sec) the subsequent reaction provides considerable insight into the kinetics of B/H/O/C/F mixtures. The present reaction mechanism allows for recombination of atomic species to yield the diatomics BO, BF, HF, OH, O_2 and H_2. It is the subsequent reaction of these diatomics with excess initial reactants which is of primary interest here. Species mole fraction profiles for the initial conditions listed in Table 8 are displayed in Figures 7 - 11.

Table 8 - Initial Conditions for Isothermal Calculations

			Species Mole Fractions				
Run #	T (k)	P (atm)	B	F	O	H	N2
1	2500	1.0	0.01	0.01	0.01	0.0	0.970
2	2500	1.0	0.01	0.02	0.005	0.0	0.965
3	2500	1.0	0.01	0.005	0.02	0.0	0.965
4	2500	1.0	0.01	0.02	0.005	0.01	0.955
5	2500	1.0	0.01	0.005	0.02	0.01	0.955

Figure 7 displays the model results for run # 1 in Table 8. For this case, there is no hydrogen in the system and the O/B and F/B mole ratios are both unity. The results indicate the

initial formation of BO and BF (occurring on the order of a 1.0 msec) followed by subsequent oxidation to OBF and minor levels of BO_2 and B_2O_3. The reaction times for the formation of BO_2 and B_2O_3 are longer than then the time required for the formation of OBF.

Figure 8 displays the model results for run # 2 in Table 8. Run # 2 differs from run # 1 in that the O/B mole ratio has been decreased by a factor of two while the F/B mole ratio has been increased by factor of two. The significant feature of these results is the sequential formation of BF_2 and BF_3 in addition to the formation of OBF. As in Figure 7 (run # 1) a significant fraction of the BO and BF is rapidly converted to OBF. The excess fluorine results in the slower reaction sequence of BF conversion to BF_2 and its subsequent conversion to BF_3. Here, OBF and BF_3 have nearly the same equilibrium mole fractions.

Figure 9 displays the model results for run # 3 in Table 8. Run # 3 differs from run # 1 in that the O/B mole ratio has been increased by a factor of two while the F/B mole ratio has been decreased by a factor of a factor of two. The subsequent kinetics are consistent with these changes. In particular, while OBF is still a dominant product it's mole fraction is approximately a factor of two smaller than for run # 1 (Figure 7). In addition, the final levels of BO_2 and B_2O_3 have been significantly increased. As previously reported,[1,2] excess oxygen results in the oxidation sequence BO ----> BO_2 ----> to B_2O_3. This reaction sequence is predicted to be slower than OBF formation rate.

Figure 10 displays the model results for run # 4 in Table 8. Run # 4 is identical to run # 2 except that atomic hydrogen has been added to the system so that the H/B mole ratio is unity. In this case HF becomes a dominant product. Since much of the fluorine is tied up in HF, there is a reduced tendency to form BF_3 via BF_2. In addition, because of the lower levels of oxygen, most of the oxygen is tied up in the stable OBF with a small contribution from HBO. Also, in comparing Figures 8 and 10 (runs #2 and #2) it is seen that hydrogen results in the preferential reduction of BO to HBO over oxidation to BO_2.

Figure 11 displays the model results for run # 5 in Table 8. Run # 5 is identical to run # 3 except that atomic hydrogen has been added to the system so that the H/B mole ratio is unity. Thus, these results illustrate the effect of hydrogen on oxygen rich mixture of run # 3. As in Figure 10, hydrogen is seen to increase the rate at which OBF is formed. The final HF and OBF

concentrations are significantly reduced relative to those shown in Figure 10 due to the reduced initial fluorine mole fraction. Because of the presence of hydrogen and the higher level of oxygen relative to fluorine, the kinetics exhibited by this system are similar to the kinetics previous seen for B/H/O/C systems. As previously reported, the excess oxygen in the presence of hydrogen produces the reactions sequences BO --> BO_2 --> HOBO and BO --> HBO --> HBO_2. Thus, while OBF and HF are still the dominant fluorine containing products, there are also relatively high levels of HOBO and B_2O_3.

In general, these results indicate that OBF is a relatively stable oxidation product for all these systems. Additionally, these results indicate that it is formed at rates faster than boron fluorides (BF_2 and BF_3). OBF, therefore, appears to play a similar role to it's isoelectronic analogue in B/H/O/C systems, HOBO.

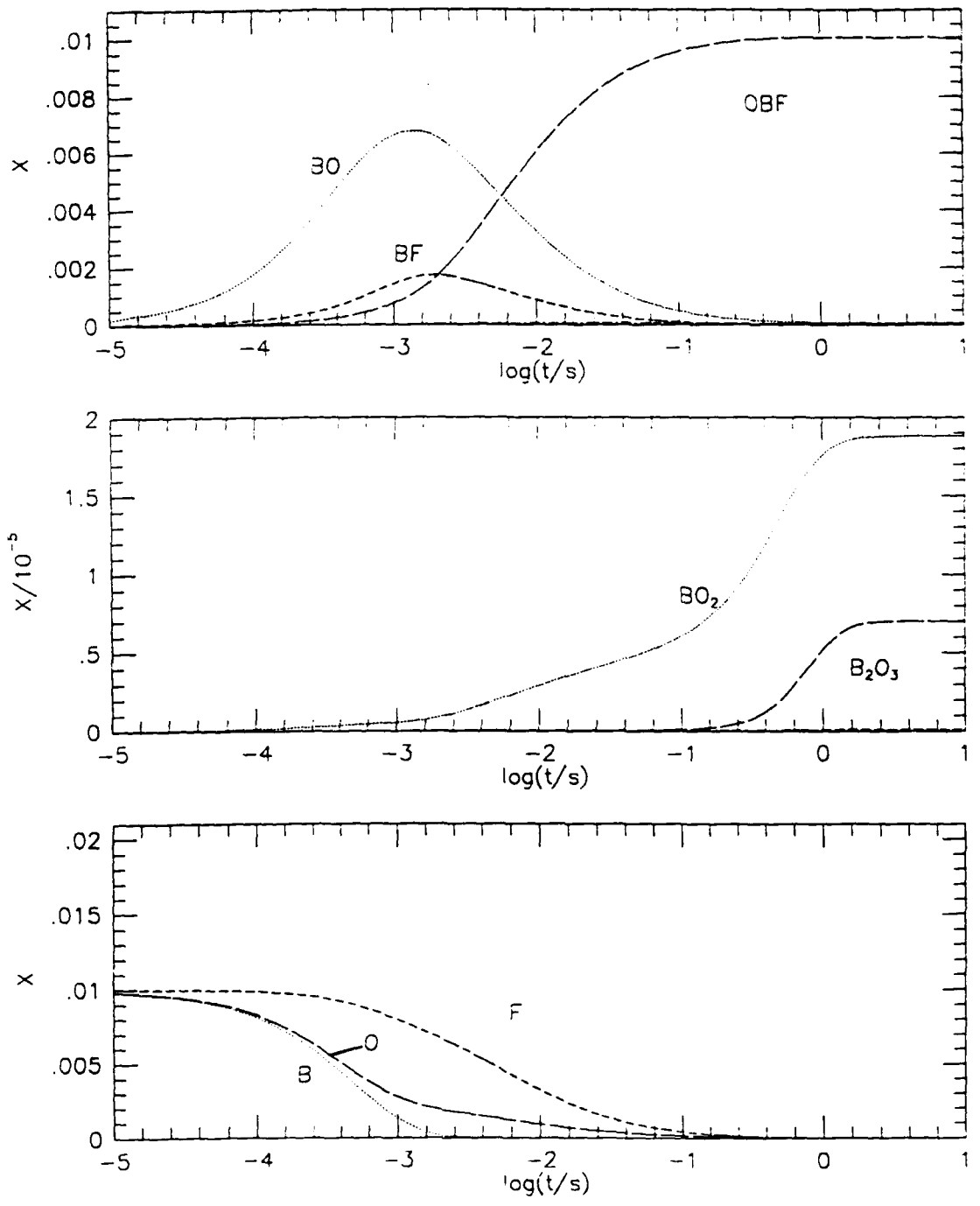

Figure 7. Species mole fractions versus time for an isothermal mixture of B(g), F(g), O(g) and N_2(g). Initial conditions: T = 2500 K, P = 1.0 atm, mole fractions X(B) = 0.01, X(F) = 0.01, X(O) = 0.01 and $X(N_2)$ = 0.97.

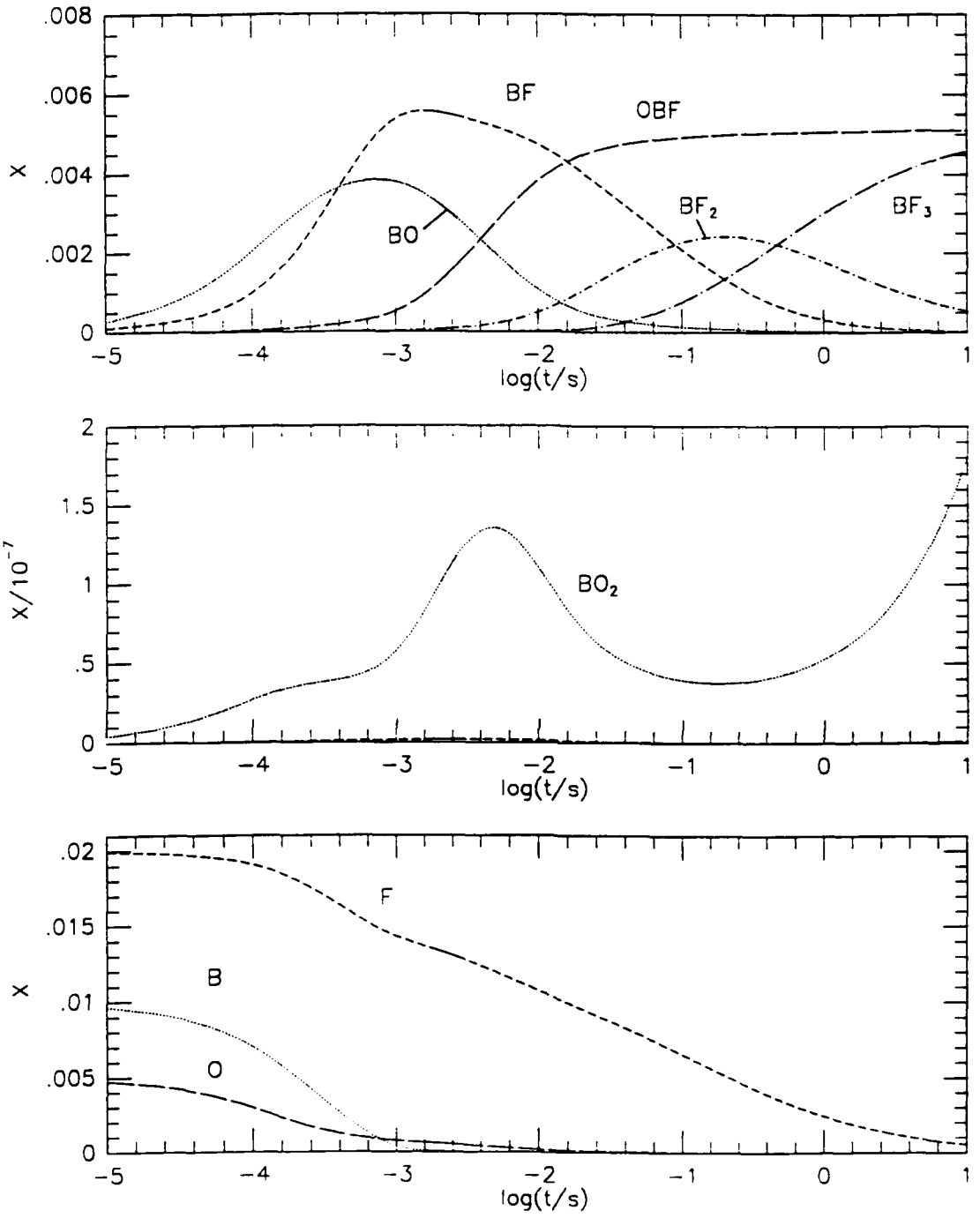

Figure 8. Species mole fractions versus time for an isothermal mixture of B(g), F(g), O(g) and N_2(g). Initial conditions: T = 2500 K, P = 1.0 atm, mole fractions X(B) = 0.01, X(F) = 0.02, X(O) = 0.005 and $X(N_2)$ = 0.965.

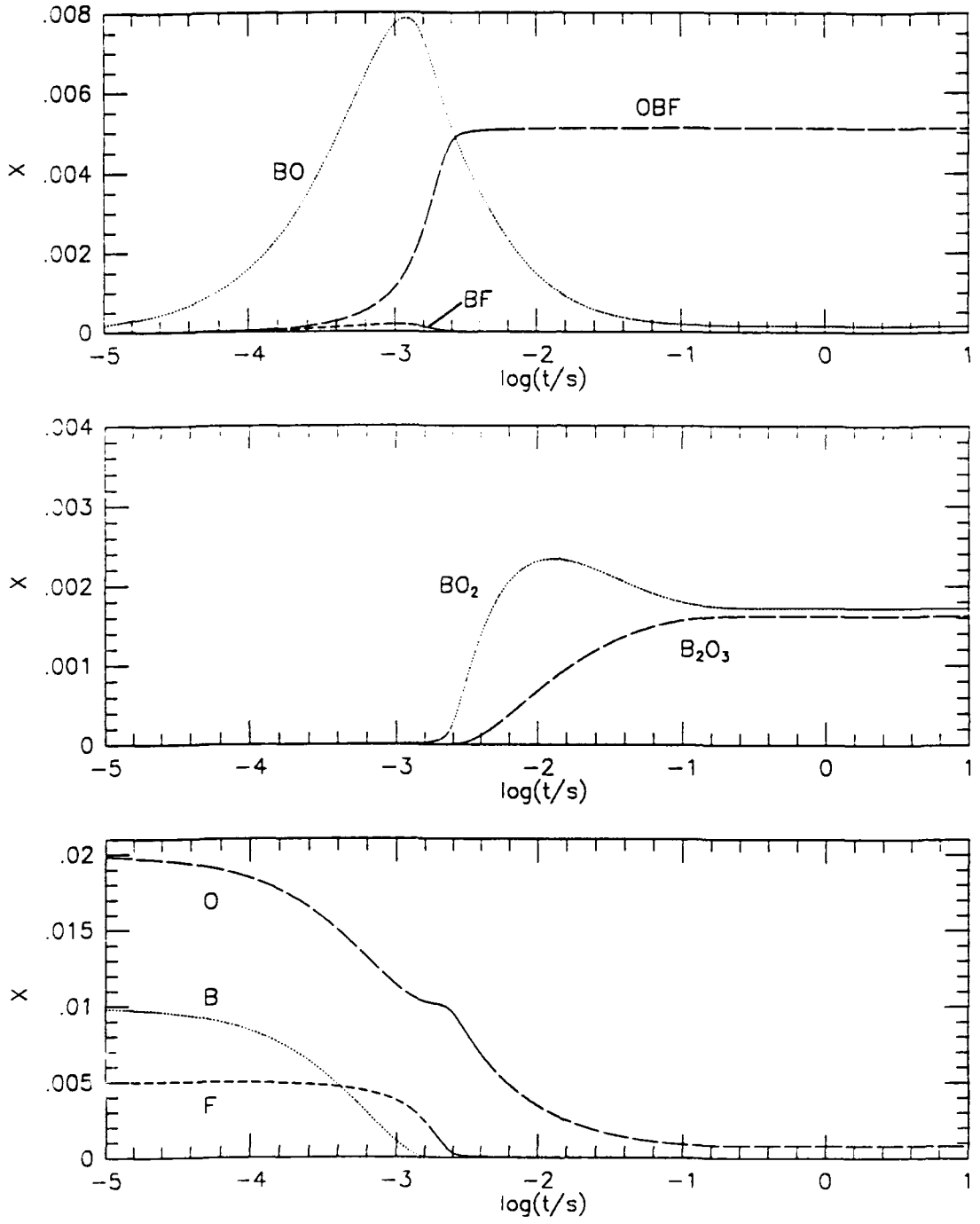

Figure 9. Species mole fractions versus time for an isothermal mixture of B(g), F(g), O(g) and N_2(g). Initial conditions: T = 2500 K, P = 1.0 atm, mole fractions X(B) = 0.01, X(F) = 0.005, X(O) = 0.02 and $X(N_2)$ = 0.965

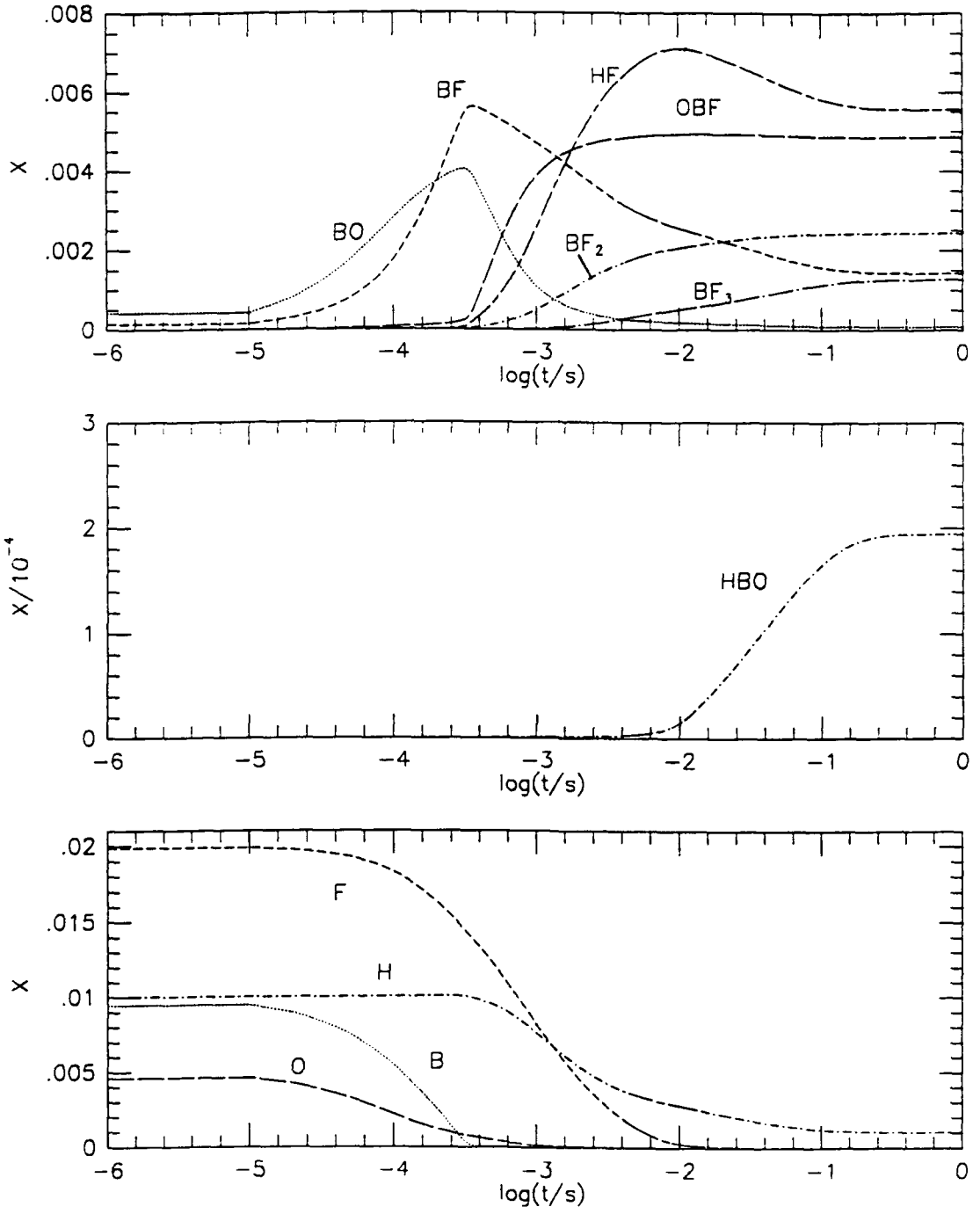

Figure 10. Species mole fractions versus time for an isothermal mixture of B(g), F(g), O(g), H(g) and N_2(g). Initial conditions: T = 2500 K, P = 1.0 atm, mole fractions X(B) =0.01, X(F) = 0.02, X(O) = 0.005, X(H) = 0.01 and $X(N_2)$ = 0.955.

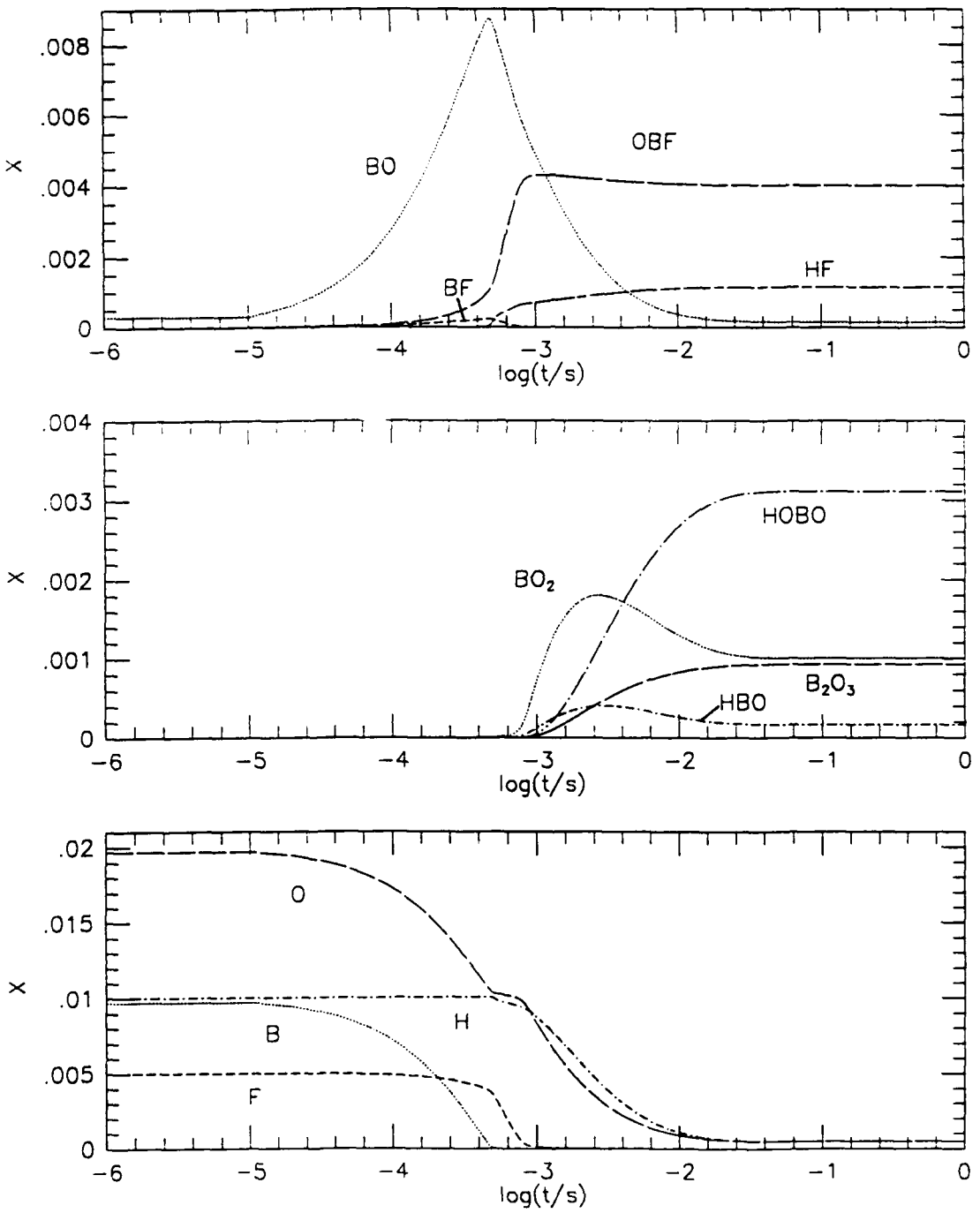

Figure 11. Species mole fractions versus time for an isothermal mixture of B(g), F(g), O(g), H(g) and N_2(g). Initial conditions: T = 2500 K, P=1.0 atm, mole fractions X(B) = 0.01, X(F) = 0.005, X(O) = 0.02, X(H) = 0.01 and $X(N_2)$ = 0.955.

4.3 Adiabatic Systems

A series of adiabatic, constant pressure kinetic calculations were preformed to illustrate the effects of O_2, H_2O and HF. Initial conditions for five separate calculations are listed in Table 9. For each run the initial mole fractions of BF, BF_2, BO, B_2O_2, OBF, CO and H_2 where fixed. This base mixture was selected to approximately represent the boundary layer speciation surrounding a boron particle. Thus, the initial conditions for boron fluorides were chosen to correspond to the equilibrium distribution described in Section 2.0 (Figure 4) for a B(s) rich mixture of B(s)/F-HMX/TMETN. BO and B_2O_2 were selected as typical surface oxidation products in oxygen environments. Various runs were then preformed by varying the initial mole fractions of O_2, H_2O and HF. The mole fraction of N_2 was adjusted for normalization.

Table 9 - Initial Conditions for Adiabatic Calculations

	Mole Fractions				
Species	Run 6	Run 7	Run 8	Run 9	Run 10
BF	0.16	0.16	0.16	0.16	0.16
BF_2	0.11	0.11	0.11	0.11	0.11
BO	0.04	0.04	0.04	0.04	0.04
B_2O_2	0.09	0.09	0.09	0.09	0.09
OBF	0.03	0.03	0.03	0.03	0.03
CO	0.04	0.04	0.04	0.04	0.04
H_2	0.04	0.04	0.04	0.04	0.04
O_2	0.13	0.00	0.00	0.13	0.13
H_2O	0.00	0.13	0.00	0.13	0.07
HF	0.00	0.00	0.13	0.13	0.13
N_2	0.36	0.36	0.36	0.10	0.16

Species mole fraction profiles are dsiplayed in Figures 12-16 for the initial conditions listed in Table 9, i.e. runs 6-10 respectively. Thus, Figure 12 (run 6) illustrates the effects of O_2, Figure 13 (run 7) illustrates the effects of H_2O, and Figure 14 (run 8) illustrates the effects of HF on the kinetics of the base mixture. Figure 15 (run 9) explores the kinetics when the base mixture is embedded in an environment consisting of equal proportions of O_2, H_2O and HF. The intial conditions for Figure 16 (run 10) are similar to those for Figure 15, except that the hydrogen concentration has been reduced by reducing the initial mole fraction of H_2O.

The results consistently show OBF as a mojor product. OBF formation is found to occur on time scales ranging from tenths to tens of microseconds. In addition, most of the heat released in these systems is associated with OBF formation. In comparison to the kinetic results shown in Figures 5 and 6 for B/H/O/C systems, it is also seen that the energy release is faster by 1-2 orders of magnitude when fluorine is present. Lastly, in comparing Figures 15 and 16, it is seen that reducing the level of hydrogen in the system results in a small decrase in the HF mole fraction and an increase in the mole fraction of OBF.

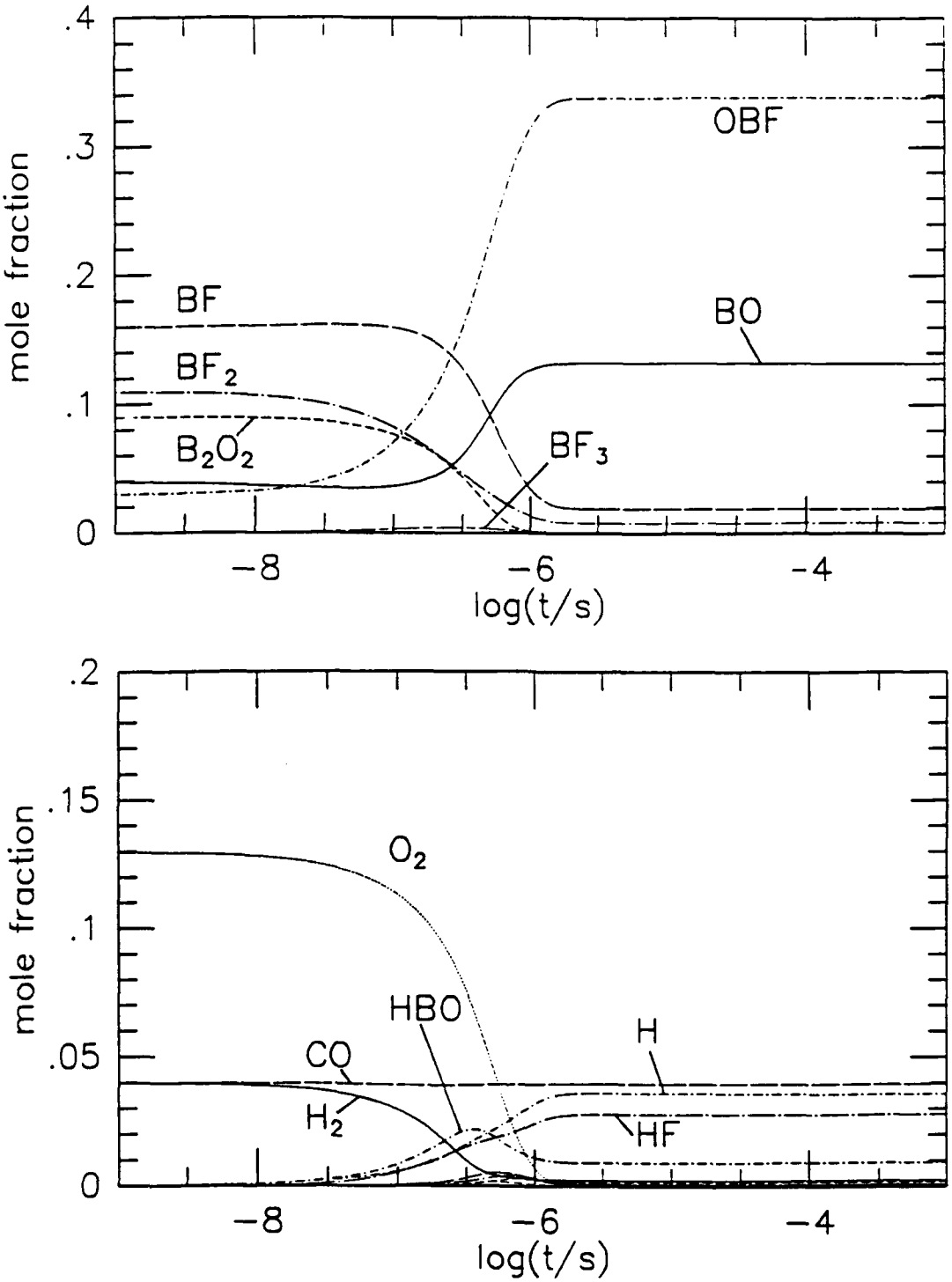

Figure 12. Species and temperature profiles for an adiabatic, constant pressure system with an initial temperature of 1800K and a pressure of 1 atm. Initial conditions: X(BF) = 0.16, $X(BF_2)$ = 0.11, X(BO) = 0.04, $X(B_2O_2)$ = 0.09, X(OBF) = 0.03, X(CO) = 0.04, $X(H_2)$ = 0.04, $X(O_2)$ = 0.13, $X(H_2O)$ = 0.0, X(HF) = 0.0, $X(N_2)$ = 0.36

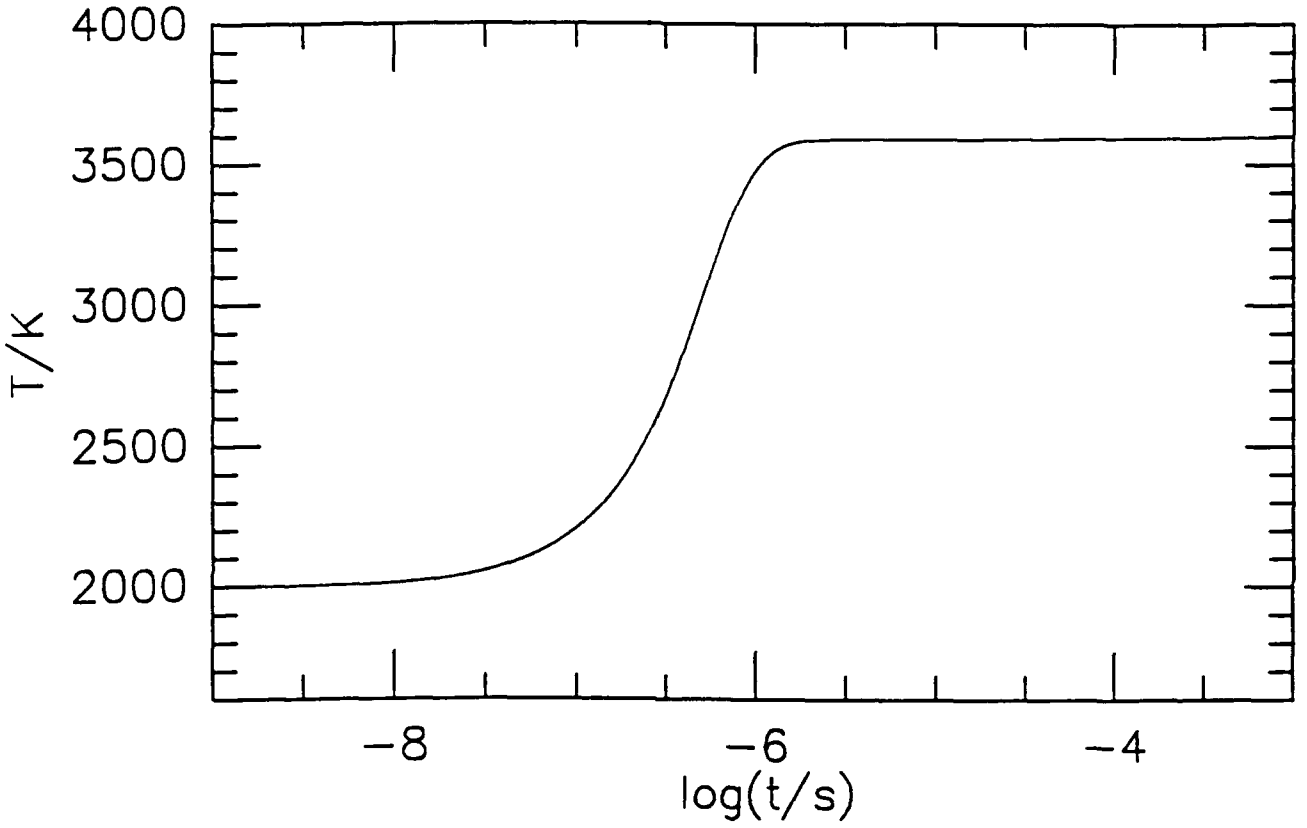

Figure 12 continued. Species and temperature profiles for an adiabatic, constant pressure system with an initial temperature of 1800K and a pressure of 1 atm. Initial conditions: X(BF) = 0.16, $X(BF_2)$ = 0.11, X(BO) = 0.04, $X(B_2O_2)$ = 0.09, X(OBF) = 0.03, X(CO) = 0.04, $X(H_2)$ = 0.04, $X(O_2)$ = 0.13, $X(H_2O)$ = 0.0, X(HF) = 0.0, $X(N_2)$ = 0.36

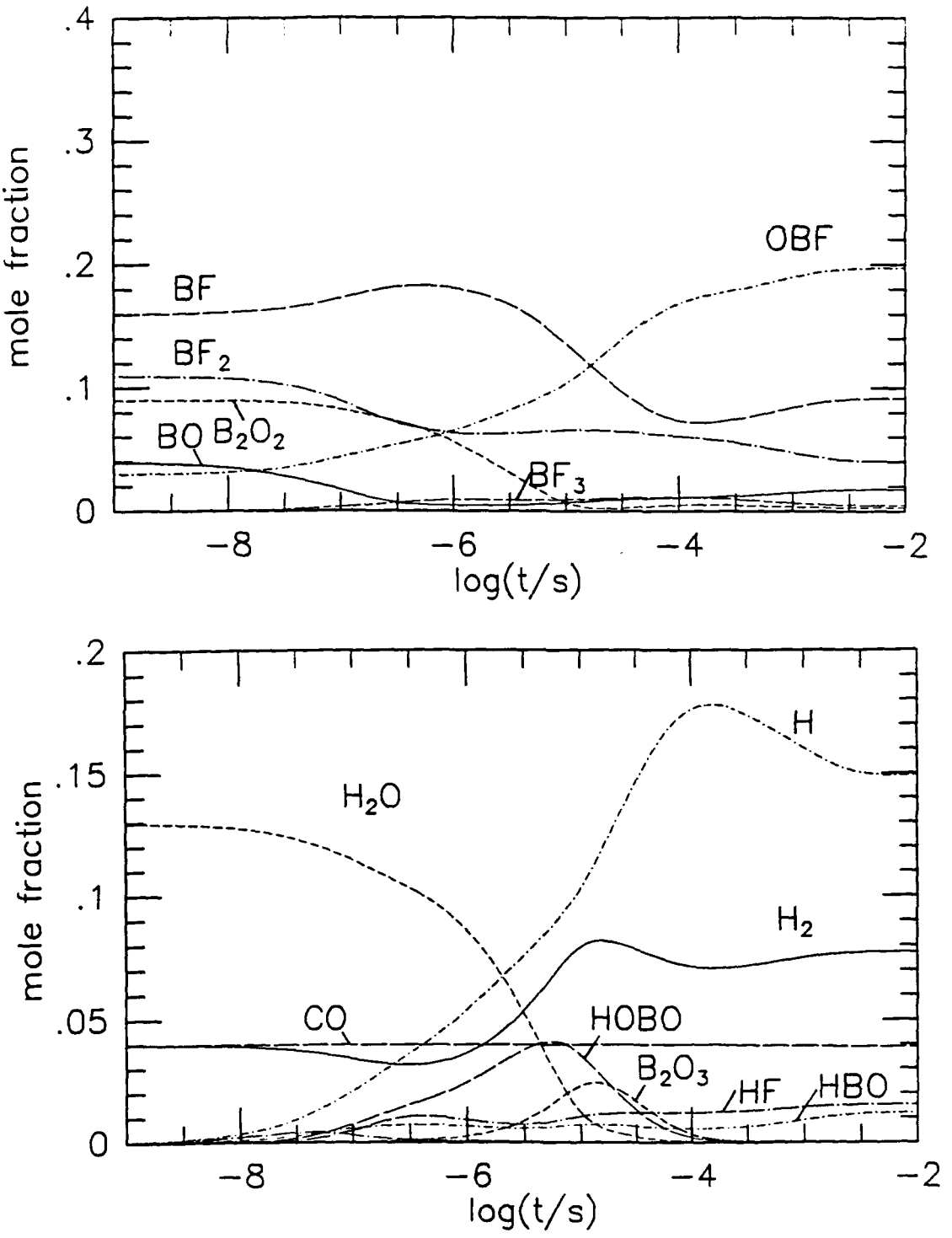

Figure 13. Species and temperature profiles for an iadiabatic, constant pressure system an initial temperature of 1800K and a pressure of 1 atm. Initial conditions: X(BF) = 0.16, X(BF_2) = 0.11, X(BO) = 0.04, X(B_2O_2) = 0.09, X(OBF) = 0.03, X(CO) = 0.04, X(H_2) = 0.04, X(O_2) = 0.0, X(H_2O) = 0.13, X(HF) = 0.0, X(N_2) = 0.36

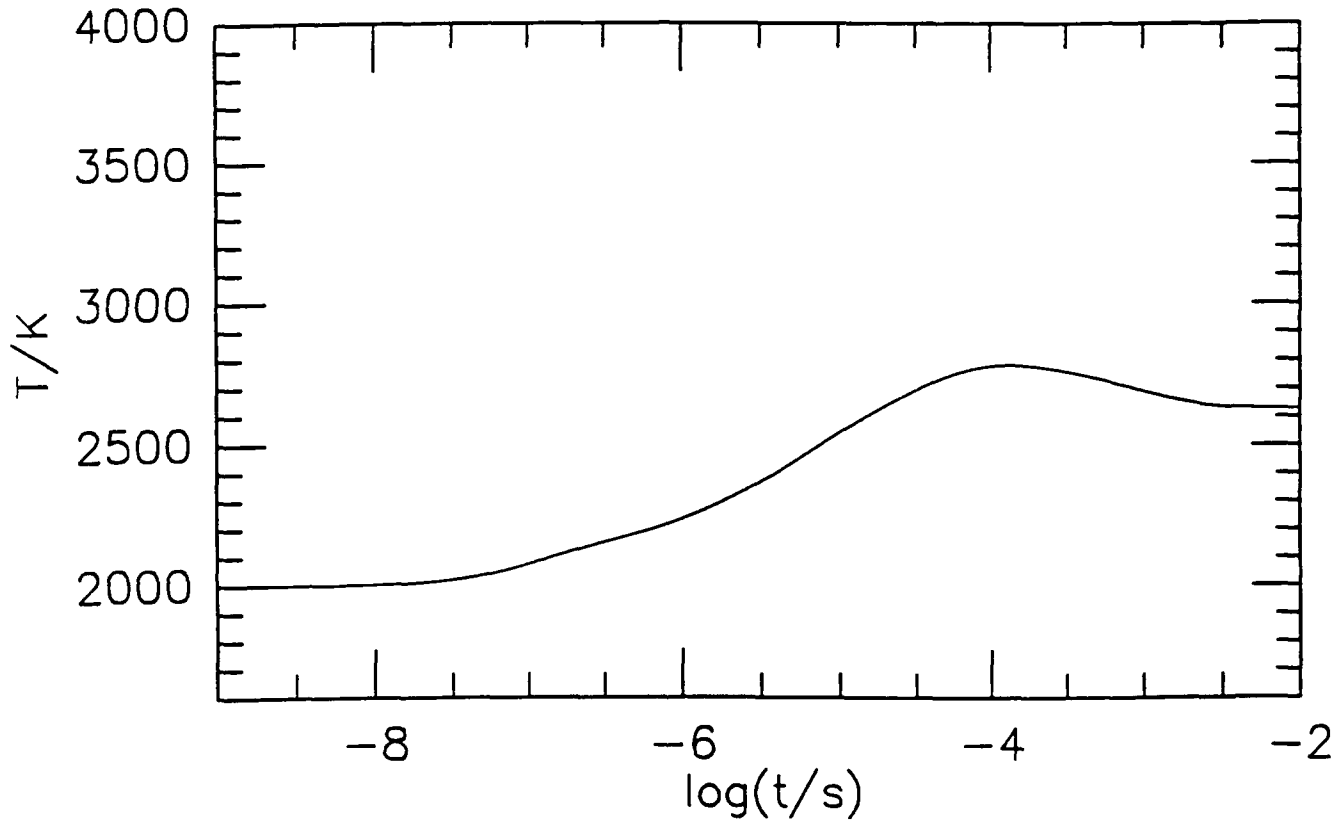

Figure 13 continued. Species and temperature profiles for an iadiabatic, constant pressure system an initial temperature of 1800K and a pressure of 1 atm. Initial conditions: X(BF) = 0.16, X(BF_2) = 0.11, X(BO) = 0.04, X(B_2O_2) = 0.09, X(OBF) = 0.03, X(CO) = 0.04, X(H_2) = 0.04, X(O_2) = 0.0, X(H_2O) = 0.13, X(HF) = 0.0, X(N_2) = 0.36

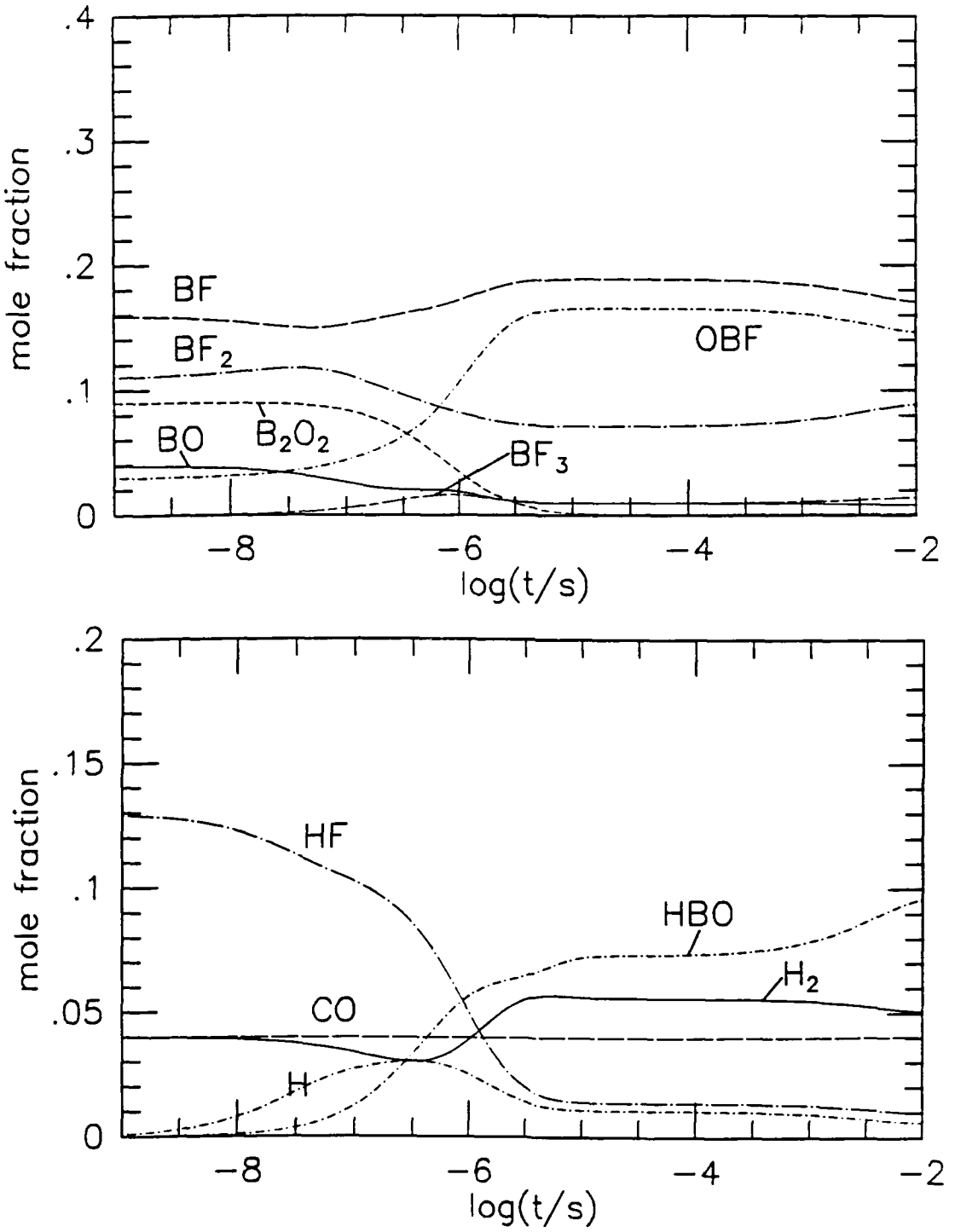

Figure 14. Species and temperature profiles for an adiabatic, constant system with an initial temperature of 1800K and a pressure of 1 atm. Initial conditions: X(BF) = 0.16, X(BF_2) = 0.11, X(BO) = 0.04, X(B_2O_2) = 0.09, X(OBF) = 0.03, X(CO) = 0.04, X(H_2) = 0.04, X(O_2) = 0.0, X(H_2O) = 0.0, X(HF) = 0.13, X(N_2) = 0.36.

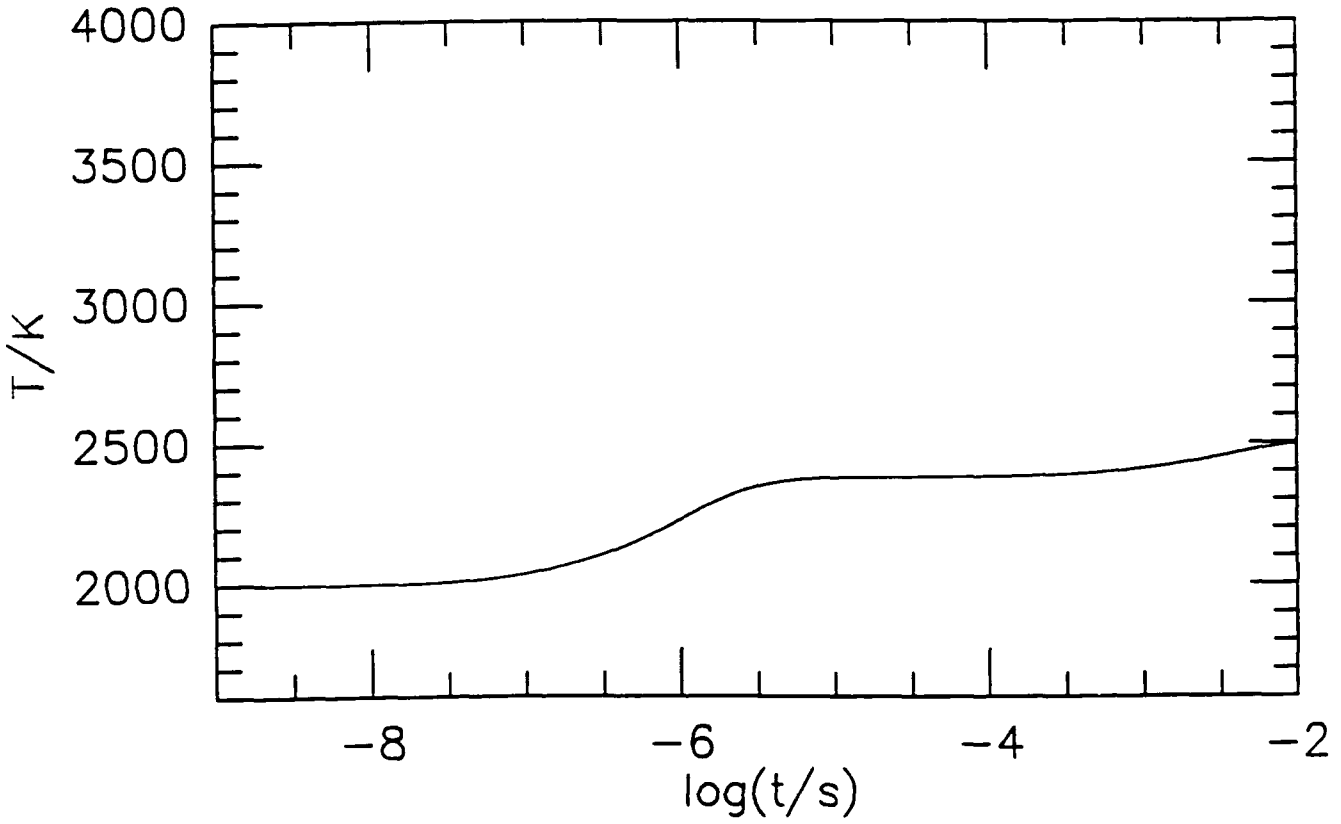

Figure 14 continued. Species and temperature profiles for an adiabatic, constant system with an initial temperature of 1800K and a pressure of 1 atm. Initial conditions: X(BF) = 0.16, $X(BF_2)$ = 0.11, X(BO) = 0.04, $X(B_2O_2)$ = 0.09, X(OBF) = 0.03, X(CO) = 0.04, $X(H_2)$ = 0.04, $X(O_2)$ = 0.0, $X(H_2O)$ = 0.0, X(HF) = 0.13, $X(N_2)$ = 0.36.

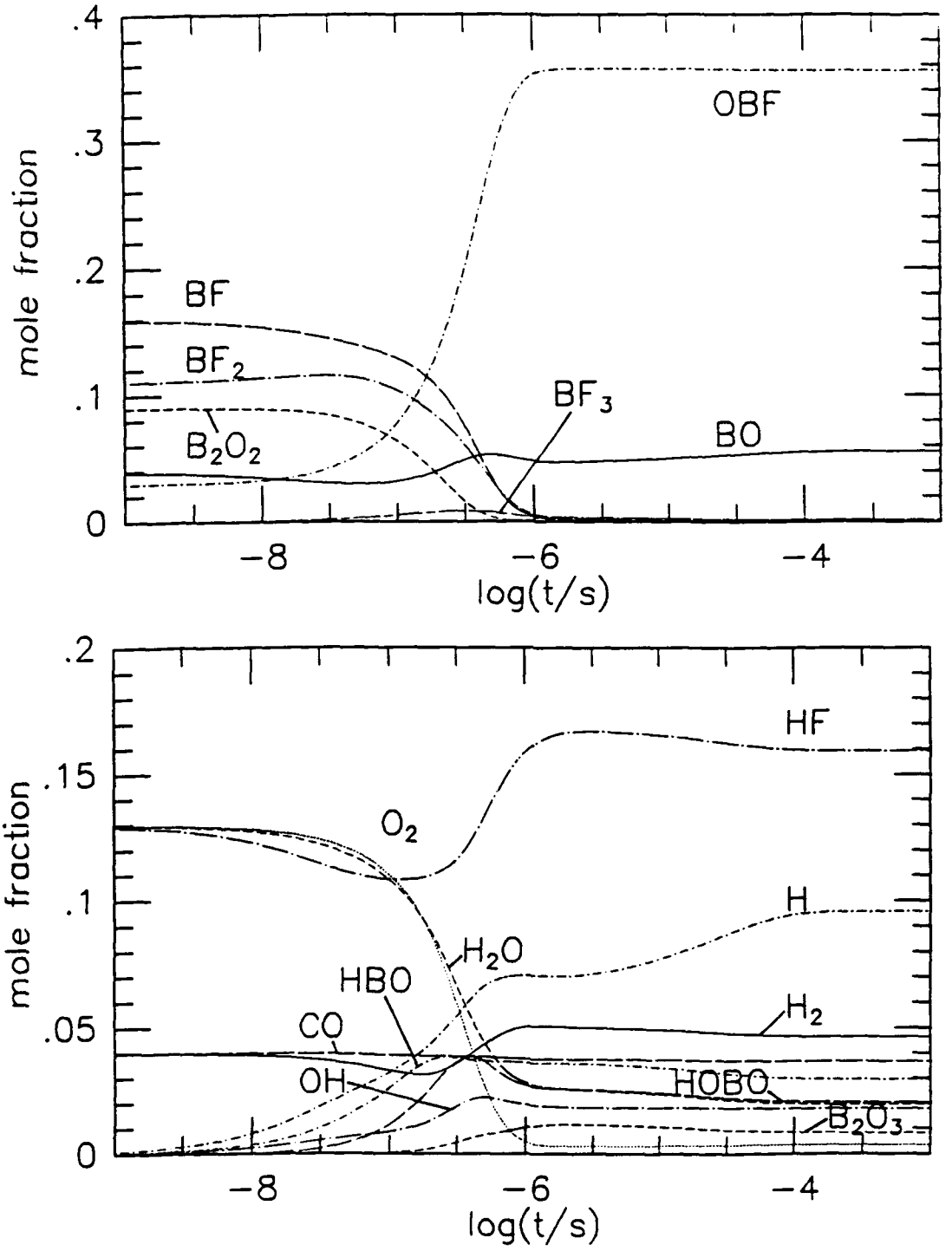

Figure 15. *Species and temperature profiles for an adiabatic, constant pressure system with an initial temperature of 1800K and a pressure of 1 atm. Initial conditions:* X(BF) = 0.16, $X(BF_2)$ = 0.11, X(BO) = 0.04, $X(B_2O_2)$ = 0.09, X(OBF) = 0.03, X(CO) = 0.04, X(H2) = 0.04, $X(O_2)$=0.13, $X(H_2O)$ = 0.13, X(HF) = 0.13, $X(N_2)$=0.13.

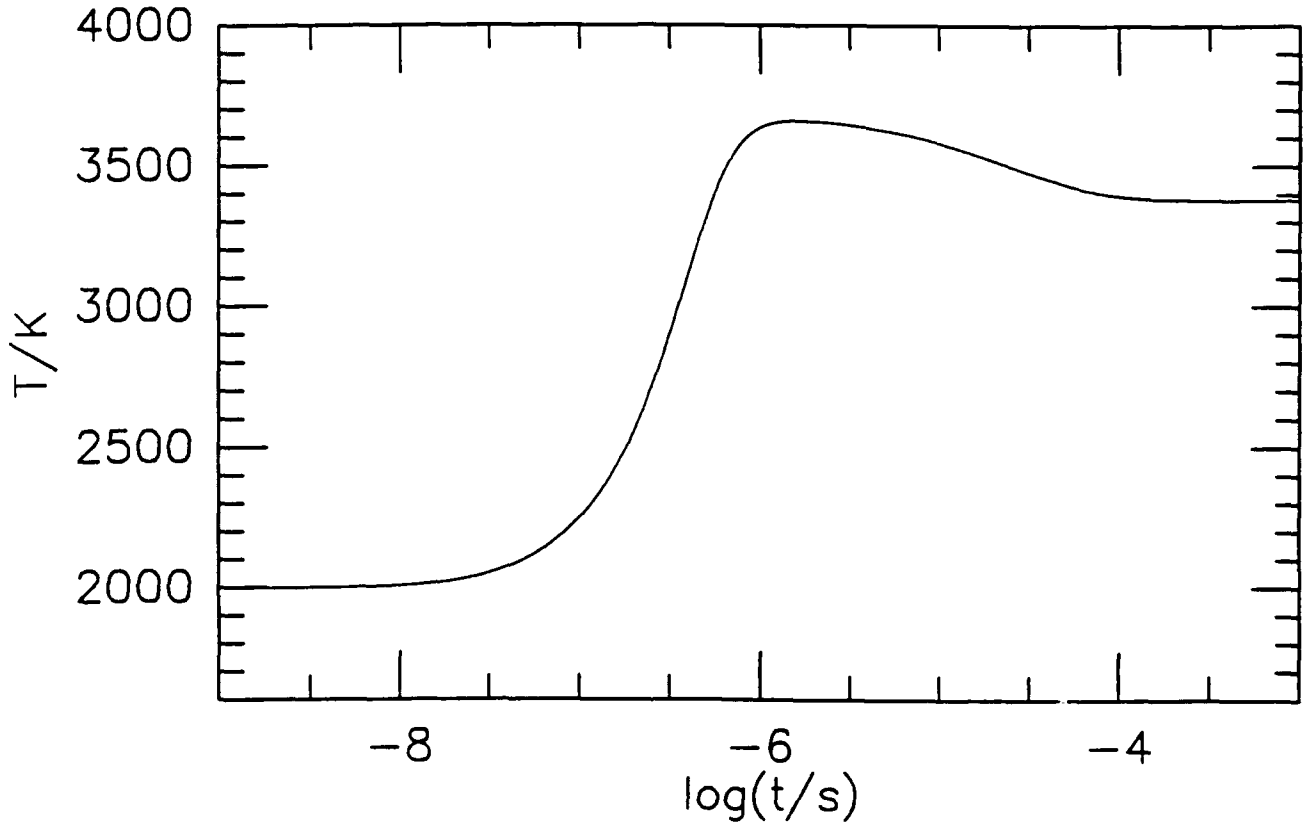

Figure 15 continued. Species and temperature profiles for an adiabatic, constant pressure system with an initial temperature of 1800K and a pressure of 1 atm. Initial conditions: X(BF) = 0.16, $X(BF_2)$ = 0.11, X(BO) = 0.04, $X(B_2O_2)$ = 0.09, X(OBF) = 0.03, X(CO) = 0.04, $X(H_2)$ = 0.04, $X(O_2)$=0.13, $X(H_2O)$ = 0.13, X(HF) = 0.13, $X(N_2)$=0.13.

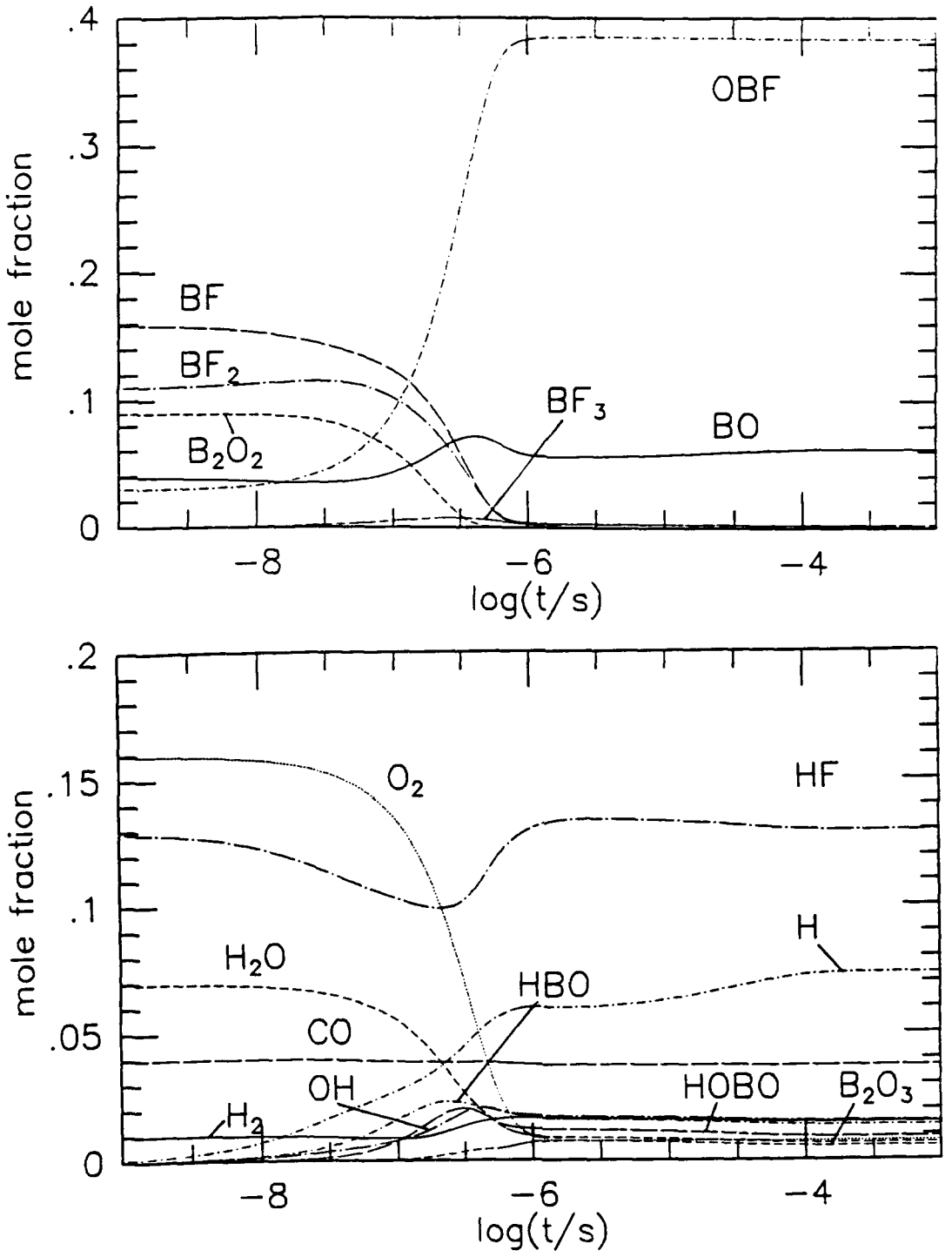

Figure 16. Species and temperature profiles for an adiabatic, constant pressure system with an initial temperature of 1800K and a pressure of 1 atm. Initial conditions: X(BF) = 0.16, $X(BF_2)$ = 0.11, X(BO) = 0.04, $X(B_2O_2)$ = 0.09, X(OBF) = 0.03, X(CO) = 0.04, $X(H_2)$ = 0.04, $X(O_2)$ = 0.13, $X(H_2O)$ = 0.07, X(HF) = 0.13, $X(N_2)$ = 0.16.

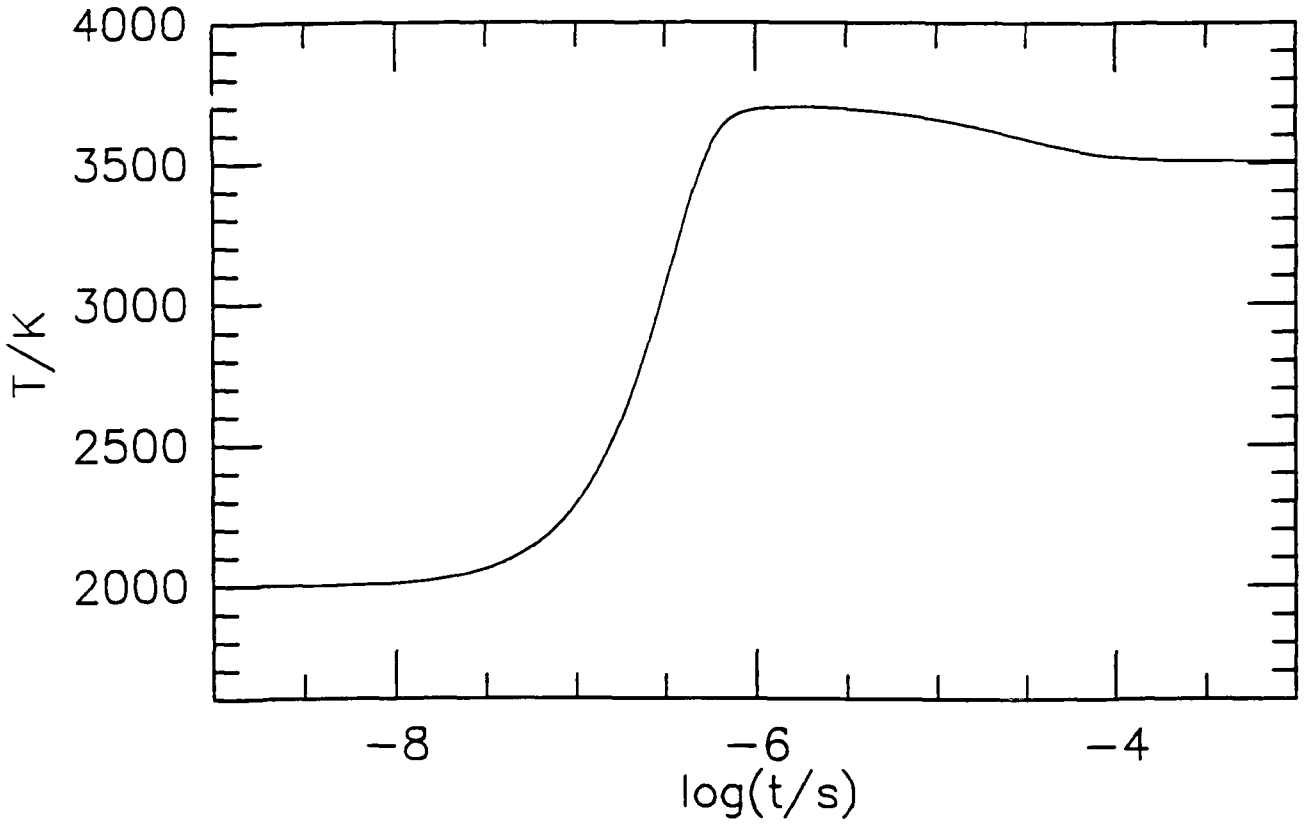

Figure 16 continued. Species and temperature profiles for an adiabatic, constant pressure system with an initial temperature of 1800K and a pressure of 1 atm. Initial conditions: X(BF) = 0.16, $X(BF_2)$ = 0.11, X(BO) = 0.04, $X(B_2O_2)$ = 0.09, X(OBF) = 0.03, X(CO) = 0.04, $X(H_2)$ = 0.04, $X(O_2)$ = 0.13, $X(H_2O)$ = 0.07, X(HF) = 0.13, $X(N_2)$ = 0.16.

5.0 REACTION FLUX AND SENSITIVITY ANALYSIS

5.1 Reaction Flux Analysis

Net reaction flux profiles (forward rate minus reverse rate) for the kinetics of Figure 11 are presented in Figures 13 - 20. This includes reactions flux profiles for OBF (Figure 13), BF and BF_2 (Figure 14), HF and BF_3 (Figure 15), BO and BO_2 (Figure 16), B_2O_2 and B_2O_3 (Figure 17), HBO and HBO_2 (Figure 18), O_2 and H_2O (Figure 19), and CO and H_2 (Figure 20).

For some reactions, fluxes are higher during initiation than during the period of reactant consumption and product formation. Hence, the magnitude of these reaction fluxes depend, in part, on the chosen initial species concentrations. The reaction flux profiles also indicate whether a particular species acts entirely as a reactant, intermediate or product. OBF, for example, is seen to be essentially an end product in all reactions involing OBF. Similarly, B_2O_2 is consumed in all reactions in which it participates.

Base on the reaction flux profiles shown in Figures 13 - 20, the fastest reactions producing and consuming the dominant species are listed in Table 10.

Table 10 - Dominant Production/Consumption Reactions from Reaction Flux Analysis

Reactant	Production	Consumption
OBF	$BF_2 + O = OBF + F$ $BF_2 + BO = OBF + BF$ $B_2O_2 + F = OBF + BO$ $BF + BO_2 = OBF + BO$ $BF + OH = OBF + H$ $F + HBO = OBF + H$ $F+ + HBO_2 = OBF + OH$ $BF + O_2 = OBF + O$	
BF	$BF_2 + BO = BF + OBF$ $BF_2 + BF_2 = BF + BF_3$	$BF + HF = BF_2 + H$ $BF + O = F + BO$ $BF + BO_2 = OBF + BO$ $BF + OH = OBF + H$
BF_2	$BF + HF = BF_2 + H$	$BF_2 + BO = OBF + BF$ $BF_2 + O = OBF + F$
BF_3	$BF_2 + BF_2 = BF_3 + BF$ $BF_2 + HF = BF_3 + H$	$BF_3 + BO = OBF + BF_2$
BO	$BF + O = BO + F$ $B_2O_2 + OH = BO + HBO_2$ $B_2O_2 + F = BO + OBF$ $BO_2 + BF = BO + OBF$ $B_2O_2 + H = BO + HBO$	$BO + H_2O = HBO + OH$ $BO + BF_2 = OBF + BF$ $BO + O_2 = BO_2 + O$ $BO + H_2 = HBO + H$
BO_2	$BO + O_2 = BO_2 + O$ $B_2O_2 + O + BO_2 + BO$	$BO_2 + BF = OBF + BO$ $BO_2 + F = OBF + O$
B_2O_2	none	$B_2O_2 + OH = HBO_2 + BO$ $B_2O_2 + F = OBF + BO$ $B_2O_2 + H = HBO + BO$ $B_2O_2 + O = BO + BO_2$
B_2O_3	$BO + HBO_2 = B_2O_3 + H$	
HBO	$BO + H_2O = HBO + OH$ $BO + H_2 = HBO + H$ $B_2O2 + H = HBO + BO$	$HBO + OH = HBO_2 + H$ $HBO + F = OBF + H$
HBO_2	$B_2O_2 + OH = HBO_2 + BO$ $HBO + OH = HBO_2 + H$	$HBO_2 + F = OBF + HBO$ $HBO_2 + BO = B_2O_3 + H$ $HBO_2 + F = HF + BO_2$

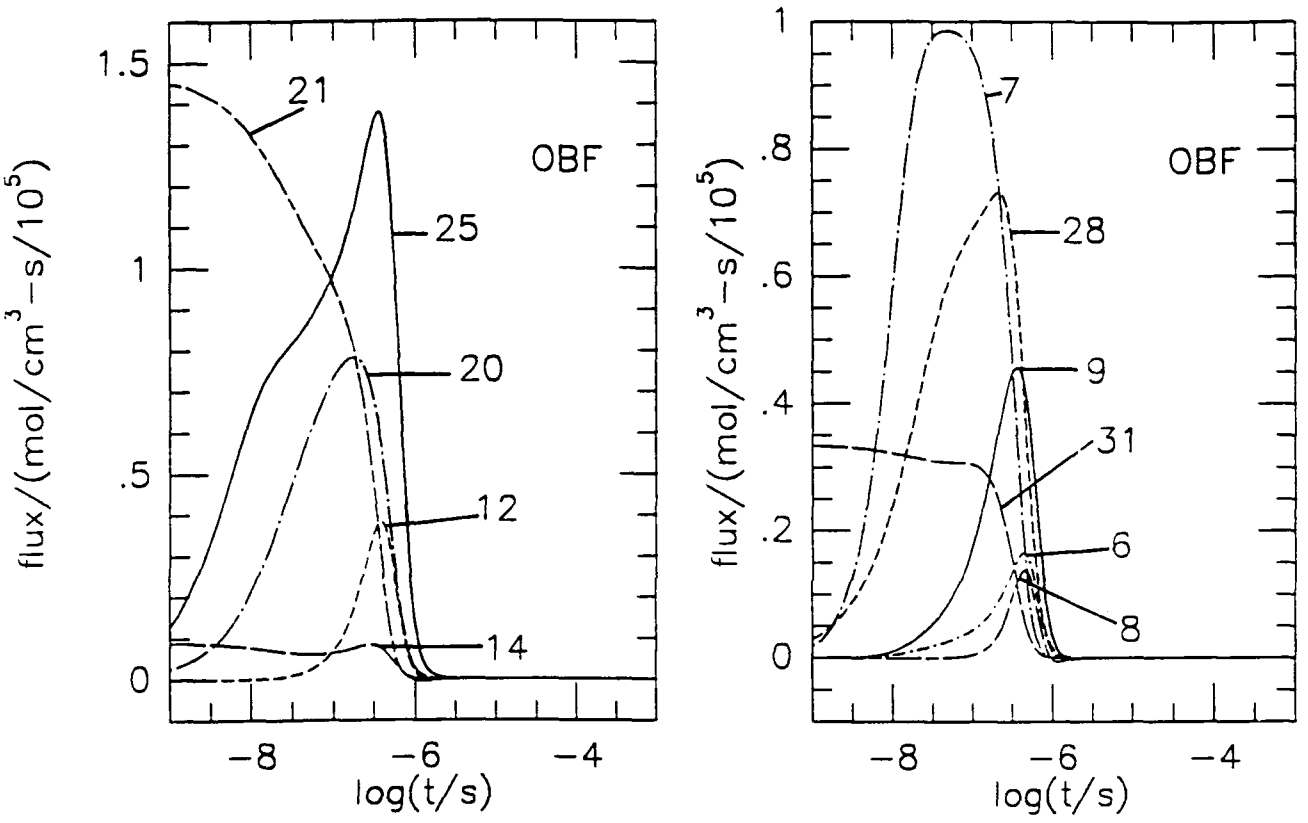

Figure 17. Reaction flux profiles of OBF. The initial conditions are the same as those of Figure 15.

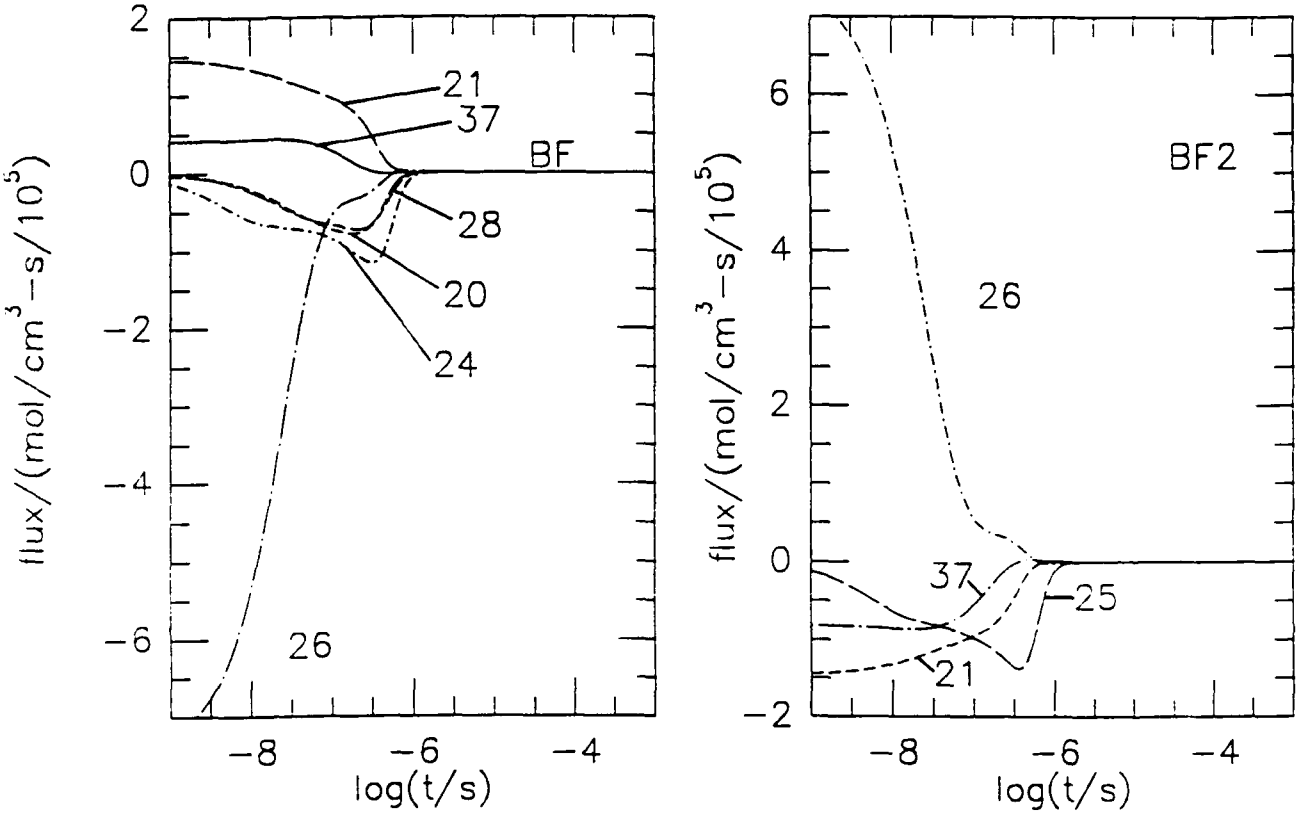

Figure 18. Reaction flux profiles for BF (part a) and BF_2 (part b). The initial conditions are the same as those of Figure 15.

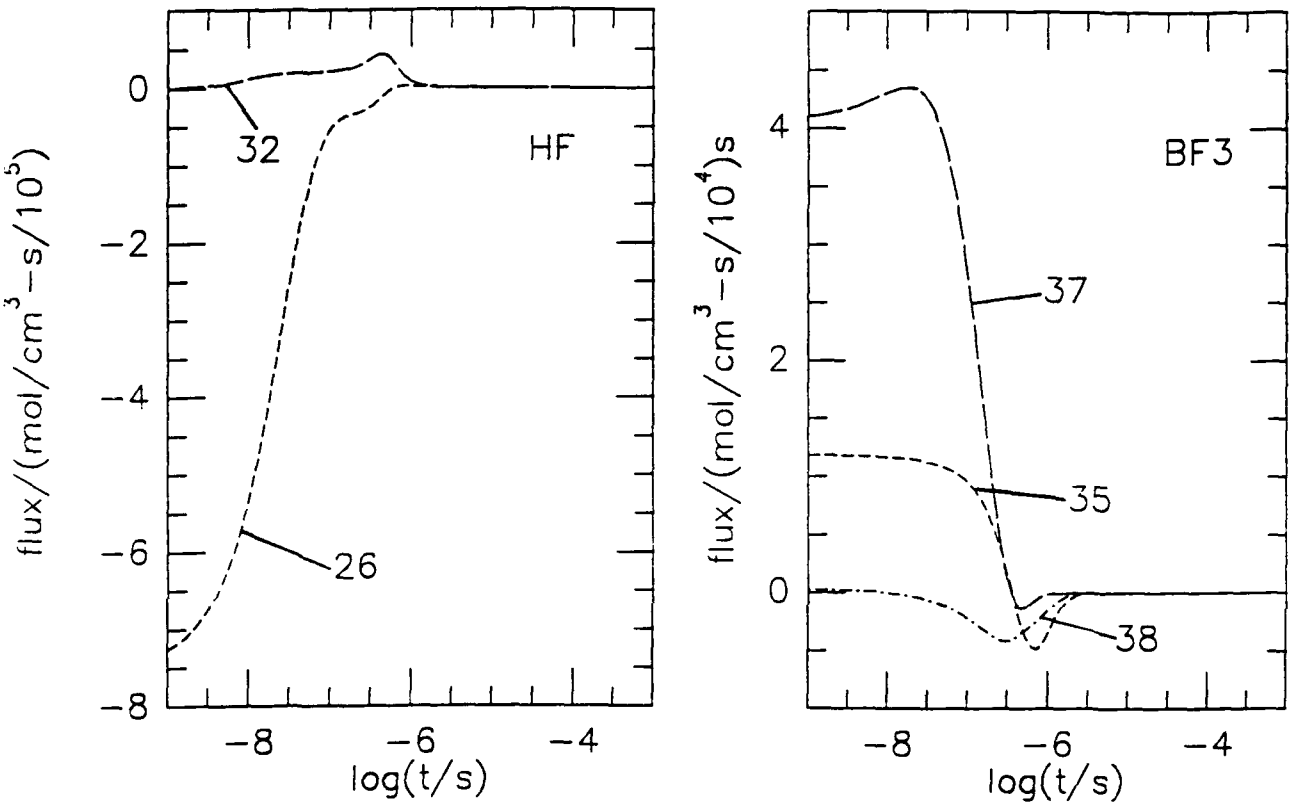

Figure 19. Reaction flux profiles for HF (part a) and BF_3 (part b). The initial conditions are the same as those of Figure 15.

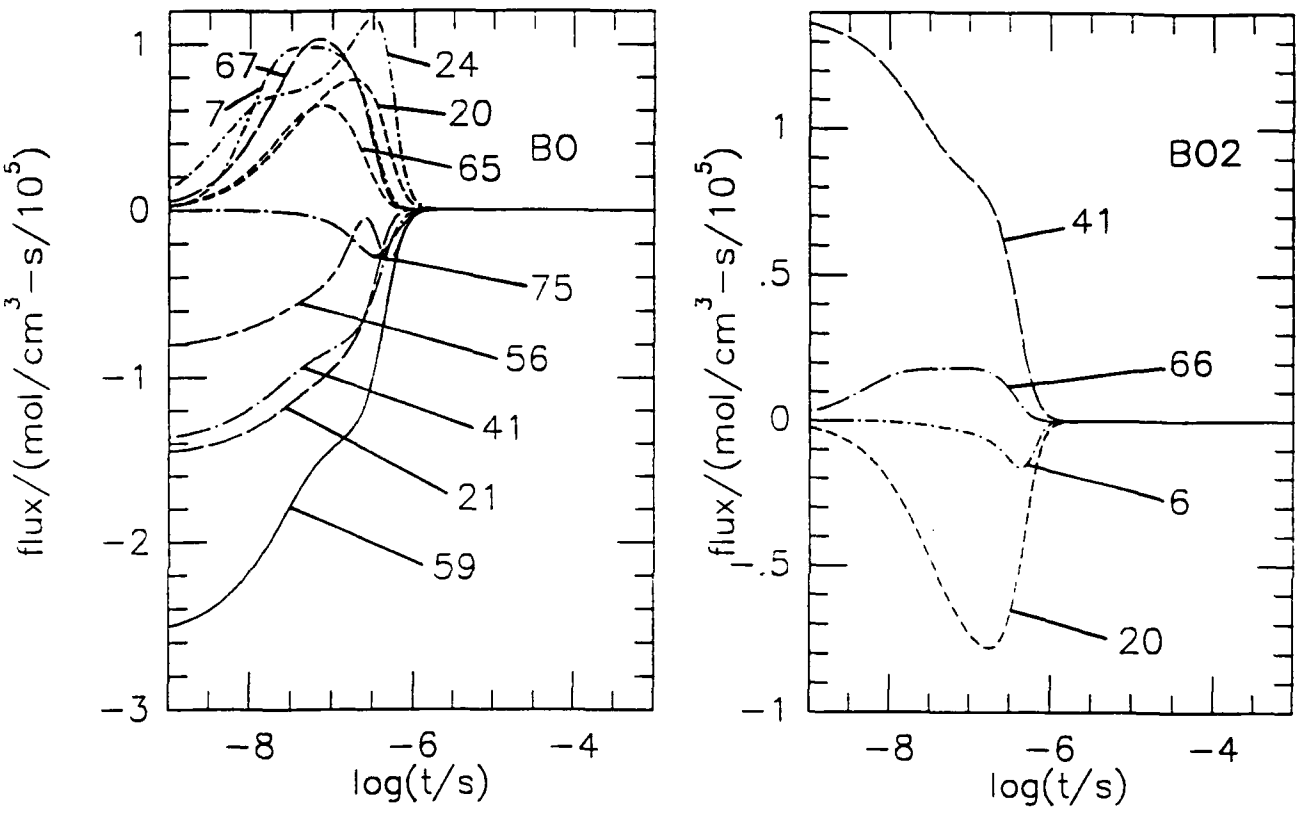

Figure 20. Reaction flux profiles for BO (part a) and BO_2 (part b). The initial conditions are the same as those of Figure 15.

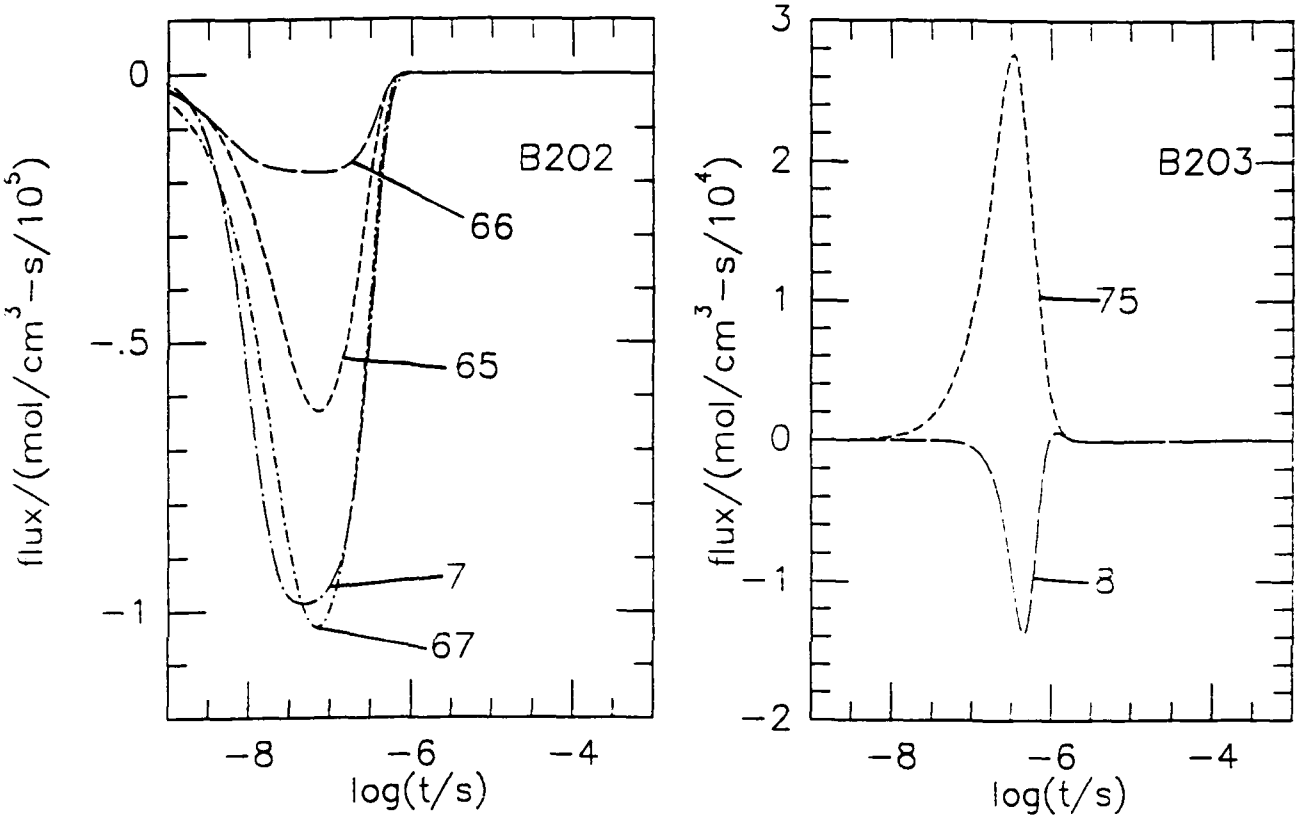

Figure 21. Reaction flux profiles for B_2O_2 (part a) and B_2O_3 (part b). The initial conditions are the same as those of Figure 15.

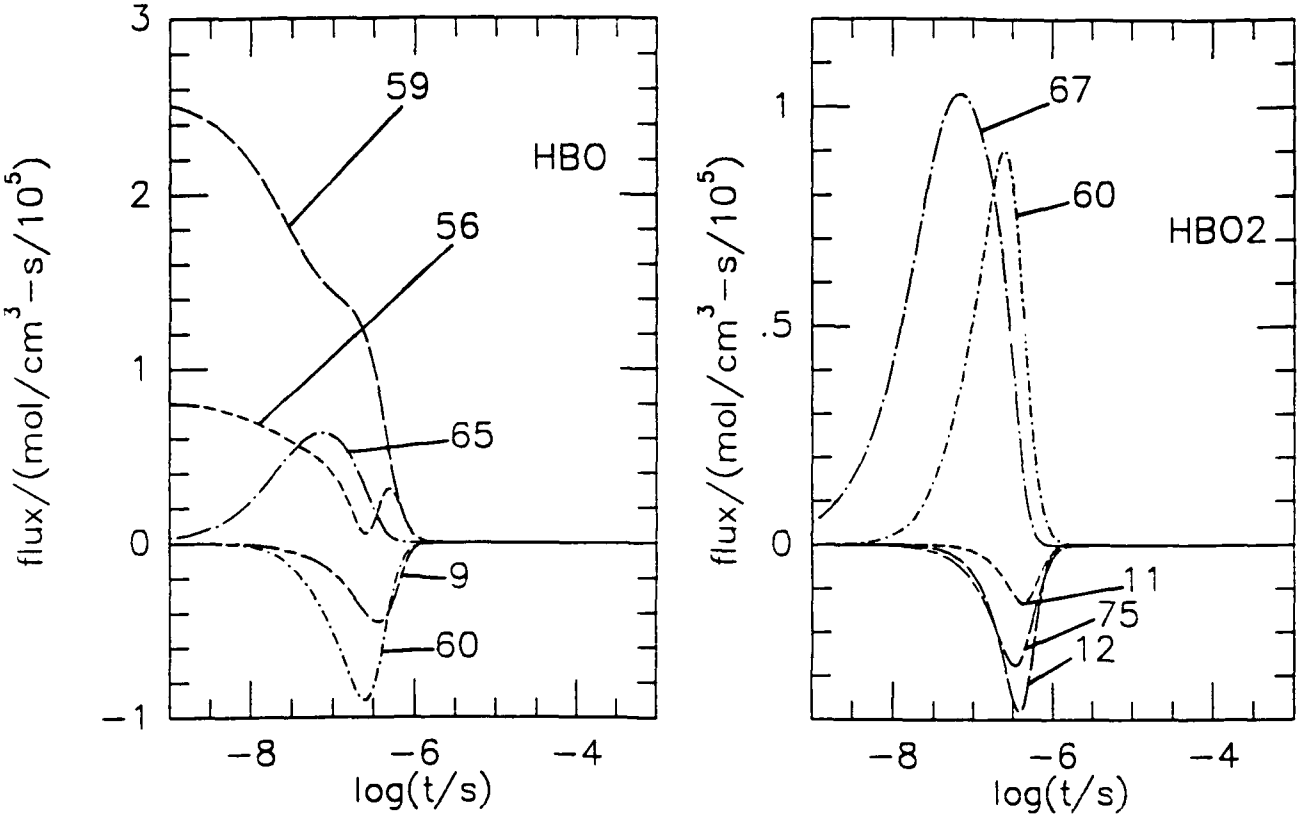

Figure 22. Reaction flux profiles for HBO (part a) and HBO_2 (part b). The initial conditions are the same as those of Figure 15.

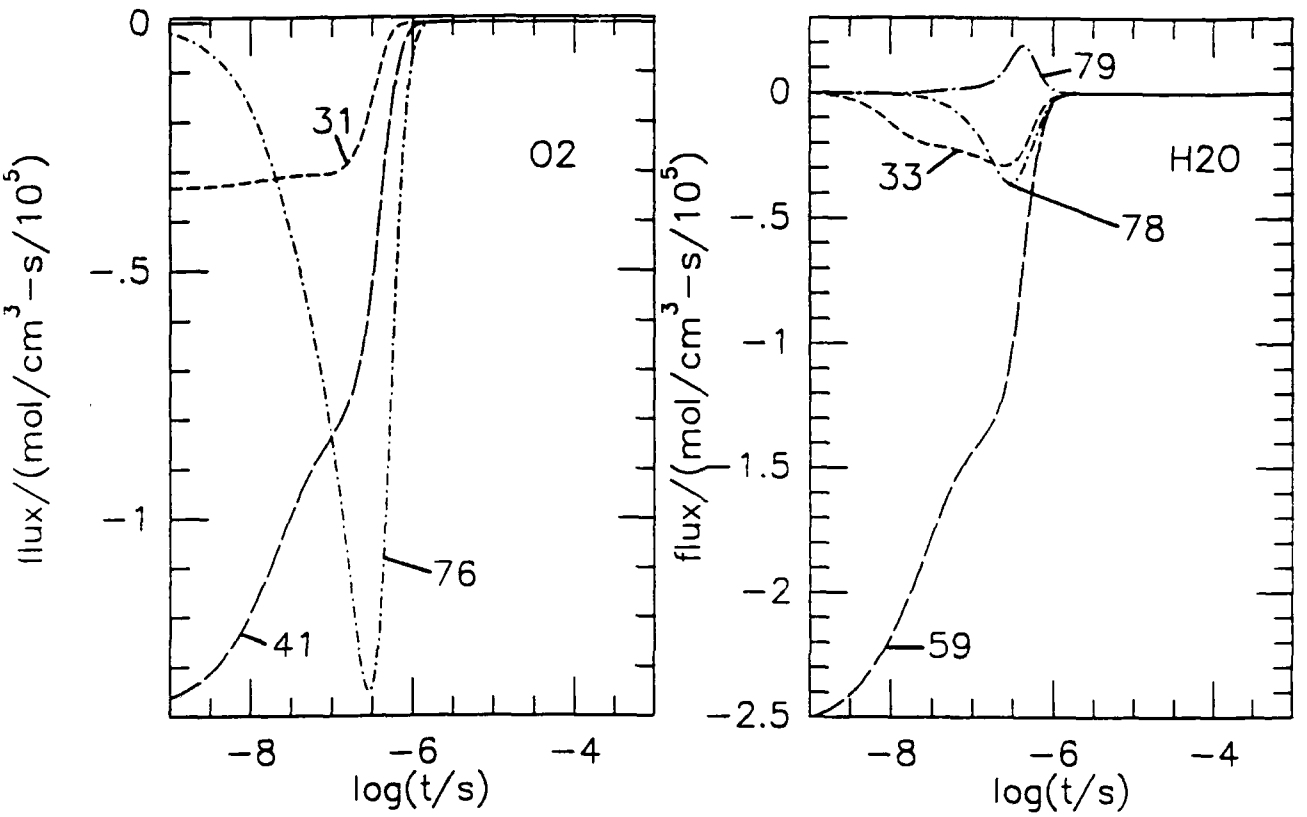

Figure 23. Reaction flux profiles for O_2 (part a) and H_2O (part b). The initial conditions are the same as those of Figure 15.

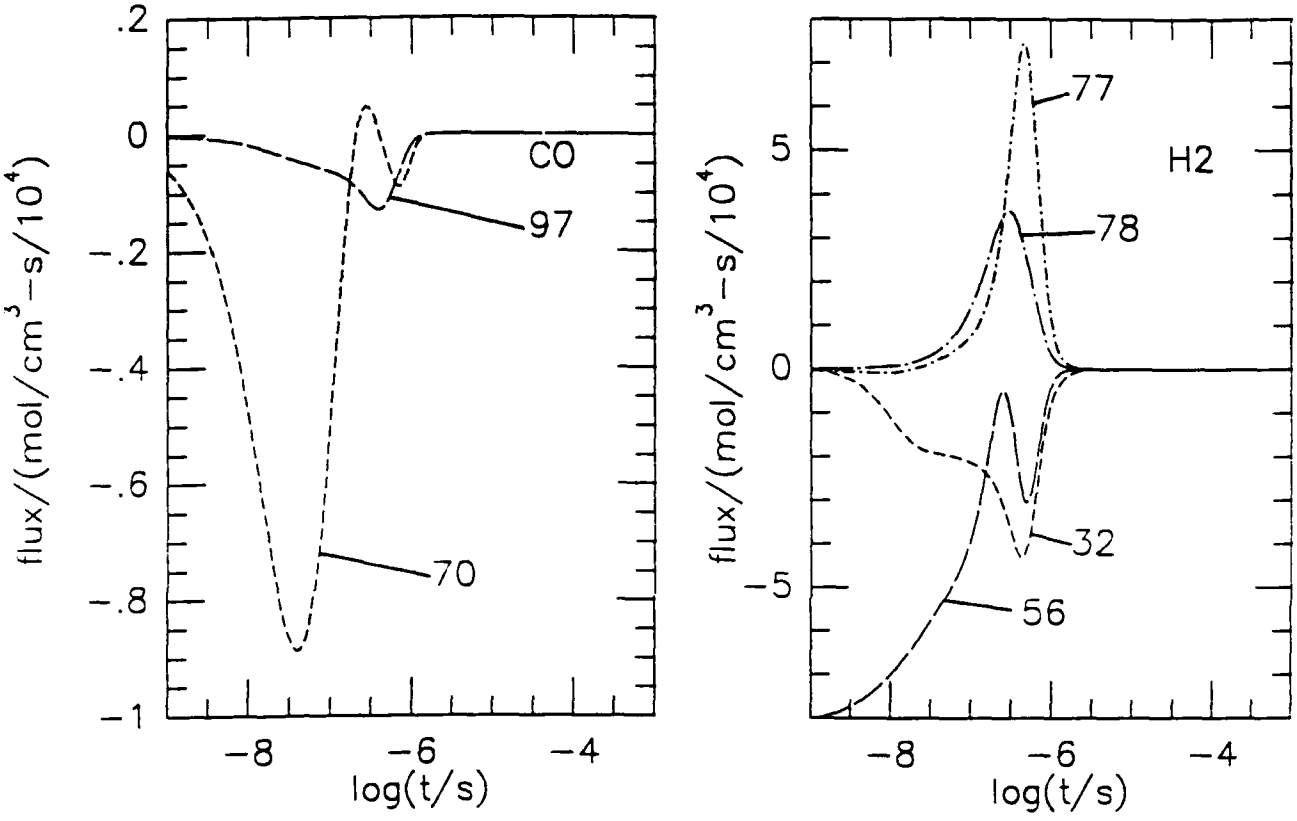

Figure 24. Reaction flux profiles for CO (part a) and H_2 (part b). The initial conditions are the same as those of Figure 15.

5.2 Gradient Sensitivity Analysis

Gradient sensitivity analysis has been preformed to identify the most important reaction pathways for the the kinetic model presented in Section 3. As an example, sensitivity gradient profiles for system designated run # 11 in Section 4.2 are displayed in Figures 21 - 27. This includes profiles for OBF (Figure 21), BF and BF_2 (Figure 22), HF and BF_3 (Figure 23), BO and BO_2 Figure (24), B_2O_2 and B_2O_3 (Figure 25), HBO and HBO_2 (Figure 26) and O_2 and H_2O (Figure 27).

The most sensitive kinetic parameters are summarized in Table 11. These reactions generally encompass the same reactions identified in the reaction flux analysis (Section 5.1), although their ranking of importance differs. This can be seen, for example, by comparing the reaction flux and sensitivity gradient profiles.

Table 11 - Important Reaction Pathways from Gradient Sensitivity Analysis

B/H/O/C/F Reactions	$B_2O_2 + F = OBF + BO$
	$HBO + F = OBF + H$
	$HBO_2 + F = OBF + OH$
	$BO_2 + BF = OBF + BO$
	$BO + BF_2 = OBF + BF$
	$BF + O = BO + F$
	$BF_2 + O = OBF + F$
	$BF_2 + H = BF + HF$
	$BF + OH = OBF + H$
	$BF + O_2 = OBF + O$
	$F + H_2 = HF + H$
	$F + H_2O + OH + HF$
	$BF_2 + HF = BF_3 + H$
	$BF_2 + BF_2 = BF_3 + BF$
	$BF_3 + BO = BF_2 + OBF$
B/H/O/C Reactions	$BO + O_2 = BO_2 + O$
	$BO + H_2 = HBO + H$
	$HBO + OH = BO + H_2O$
	$HBO + OH = HBO_2 + H$
	$B_2O_2 + H = BO + HBO$
	$B_2O_2 + O = BO + BO_2$
	$B_2O_2 + OH = BO + HBO_2$
	$BO + HBO_2 = B_2O_3 + H$
H/O/C Reactions	$H + O_2 = O + OH$
	$O + H_2 = H + OH$

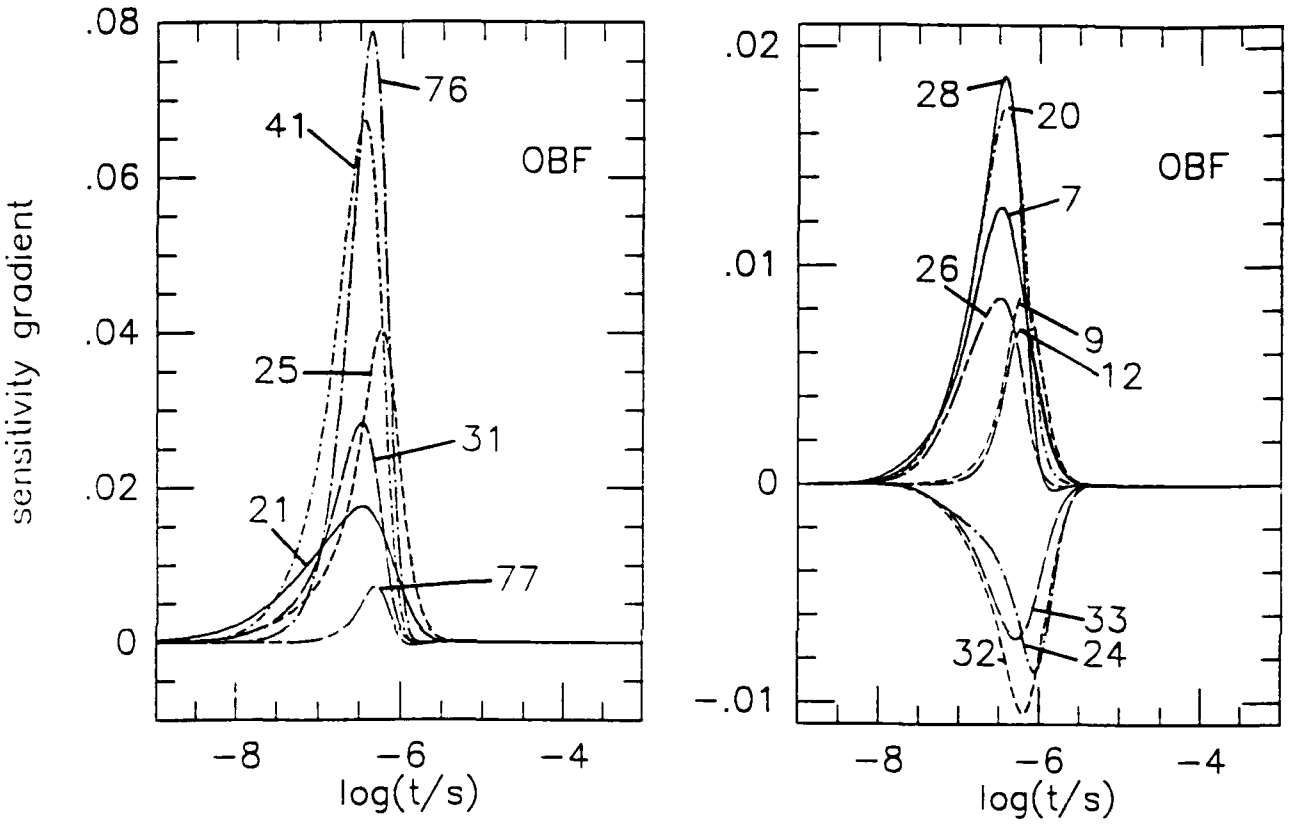

Figure 25. Sensitivity gradient profiles for OBF. The initial conditions are the same as those of Figure 15.

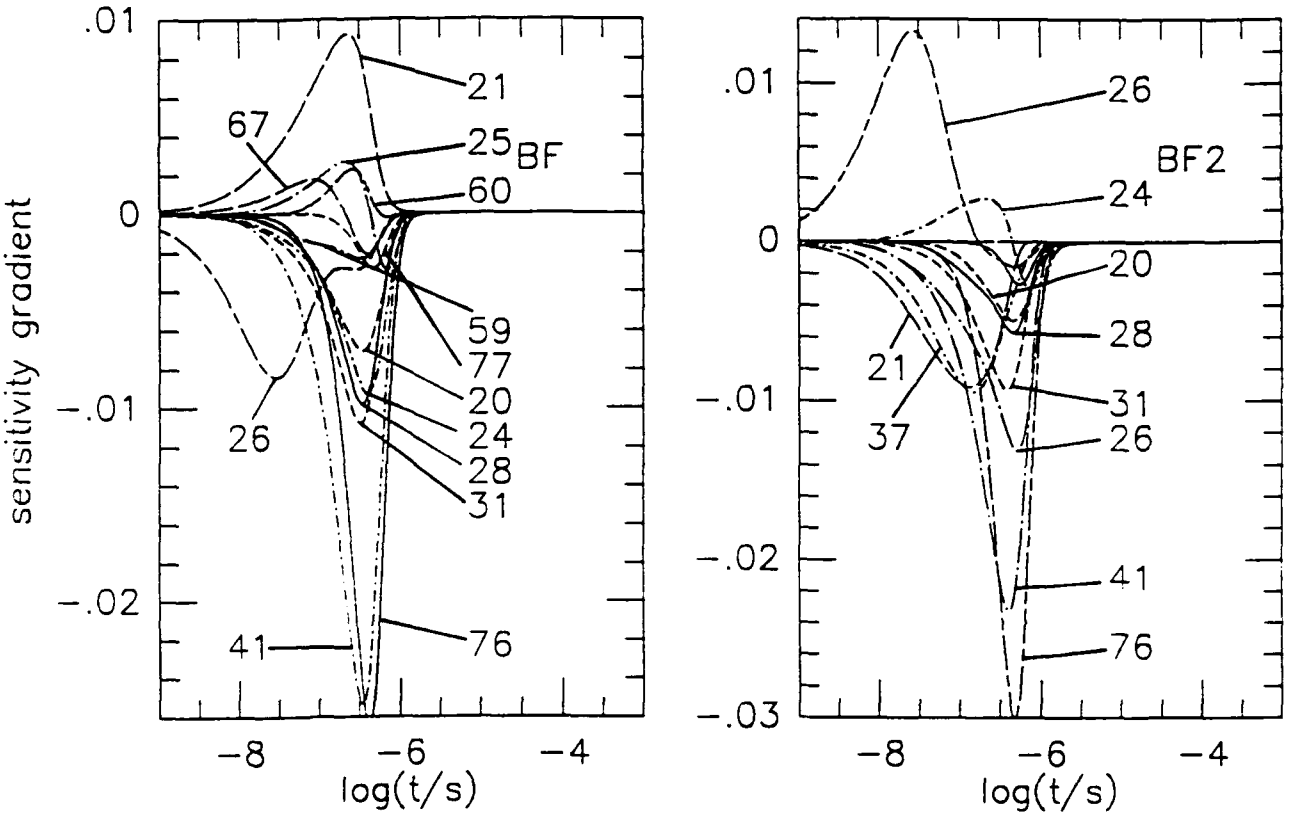

Figure 26. Sensitivity gradient profiles for BF (part a) and BF_2 (part b). The initial conditions are the same as those of Figure 15.

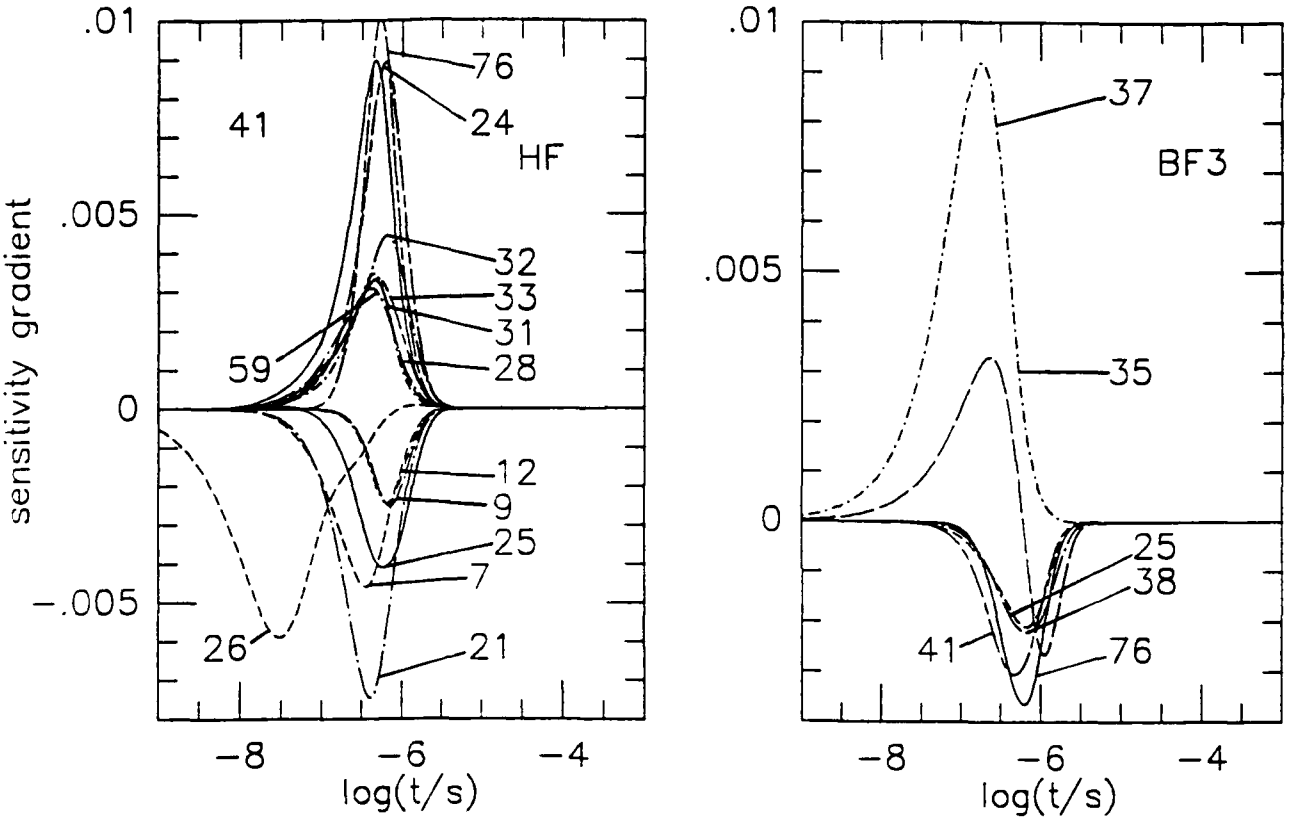

Figure 27. Sensitivity gradient profiles for HF (part a) and BF_3 (part b). The initial conditions are the same as those of Figure 15.

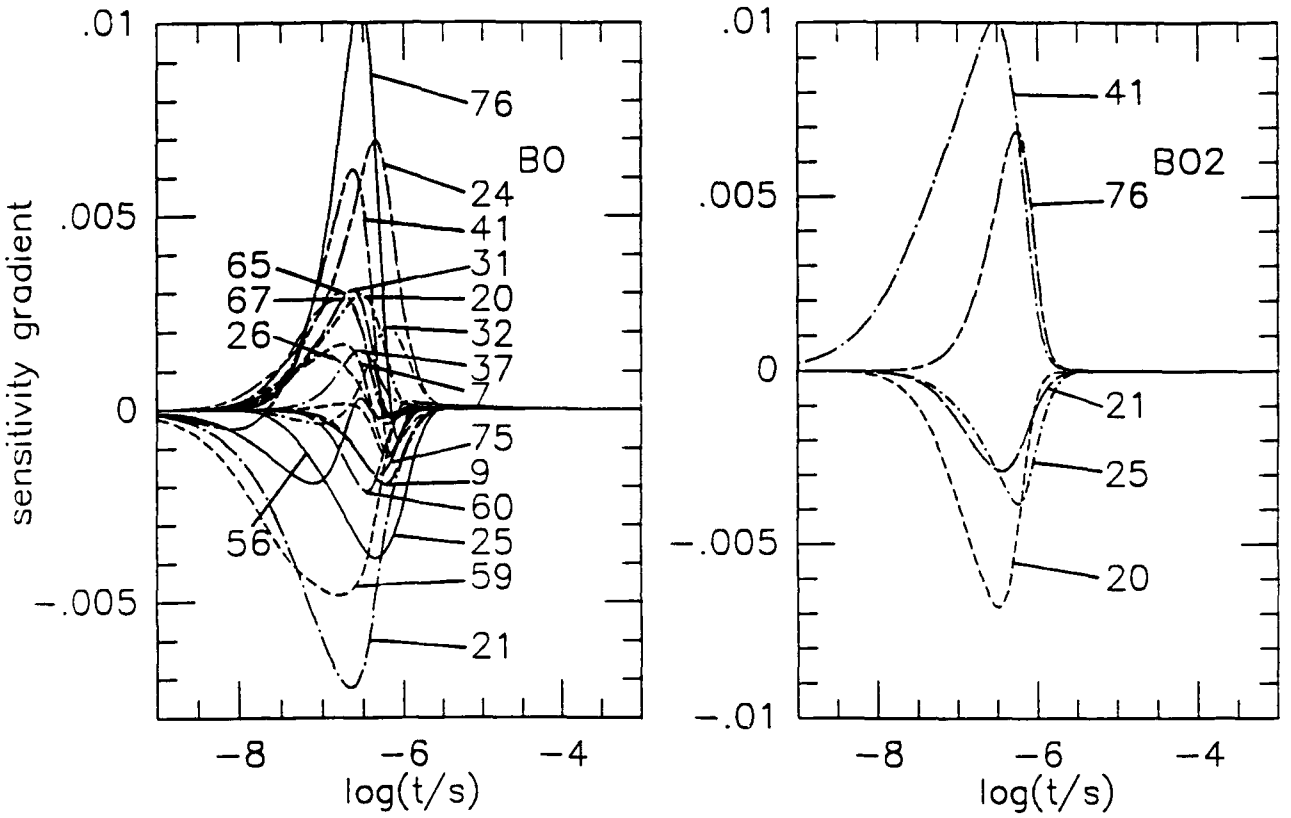

Figure 28. Sensitivity gradient profiles for BO (part a) and BO_2 (part b). The initial conditions are the same as those of Figure 15.

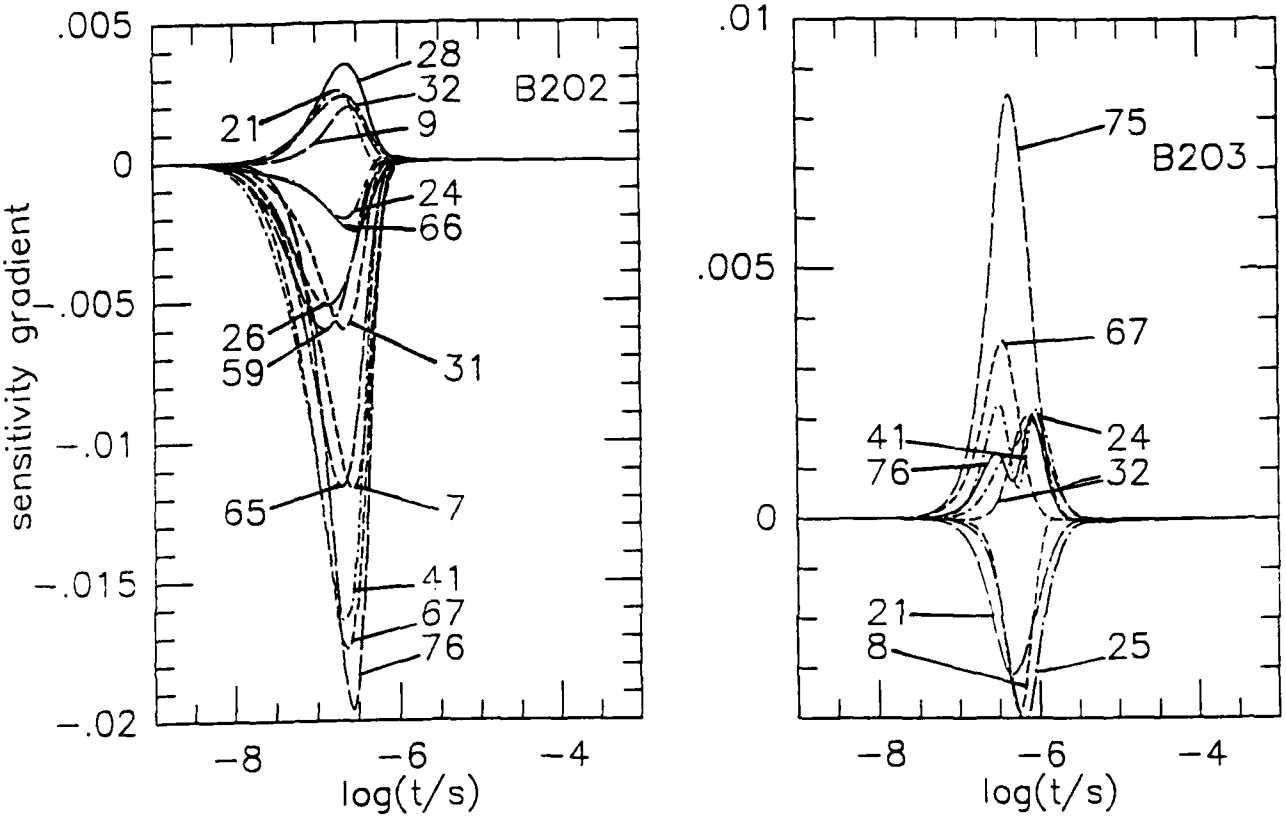

Figure 29. Sensitivity gradient profiles for B_2O_2 (part a) and B_2O_3 (part b). The initial conditions are the same as those of Figure 15.

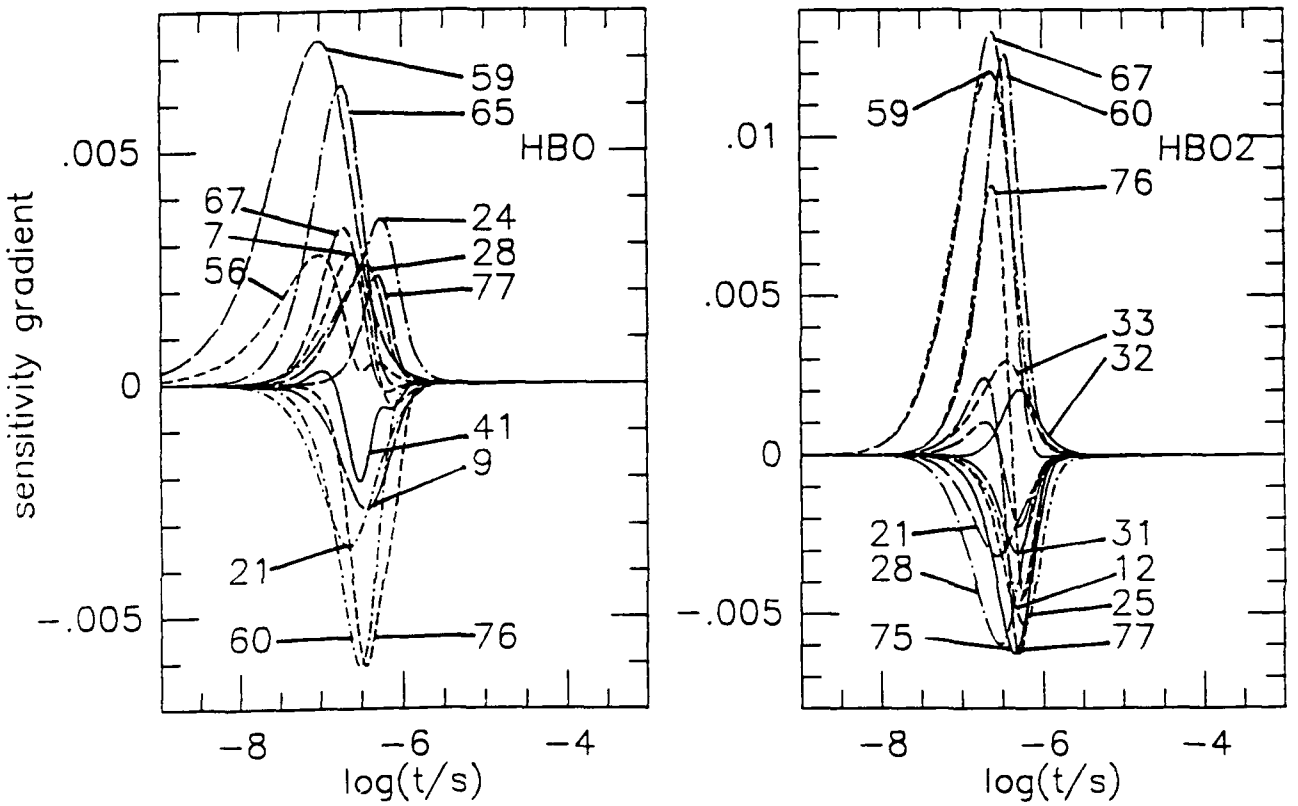

Figure 30. Sensitivity gradient profiles for HBO (part a) and HBO_2 (part b). The initial conditions are the same as those of Figure 15.

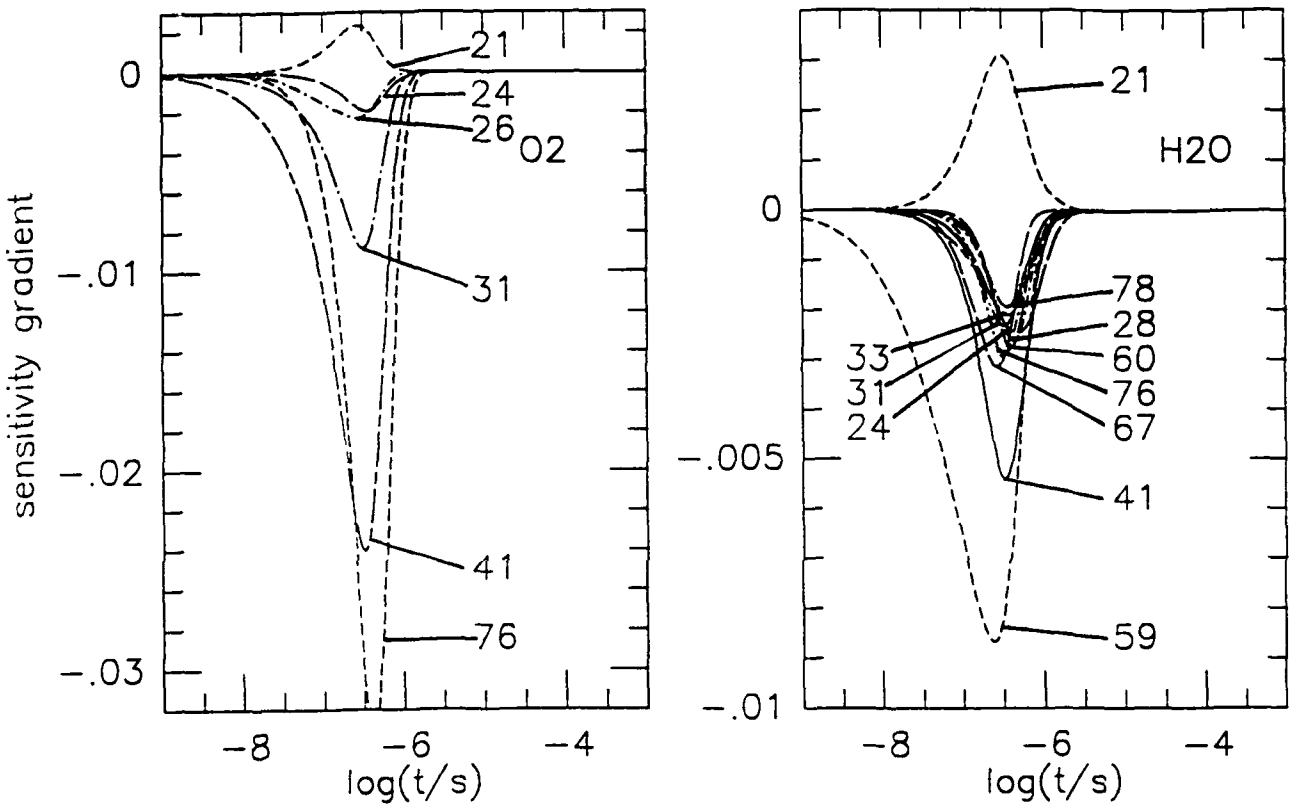

Figure 31. Sensitivity gradient profiles for O_2 (part a) and H_2O (part b). The initial conditions are the same as those of Figure 15.

6.0 SUMMARY

In this report, a gas phase kinetic model for high temperature B/H/O/C/F systems has been developed and standard reaction flux and sensitivity analysis techniques have been used to identify important reaction pathways. The model development was specifically concerned with simulating the gas phase oxidation chemistry associated with fluoroamino/nitroamino/B(s) mixtures which are currently of interest with respect to advanced underwater explosives and solid propellant ignition systems. However, the model is applicable to other systems based on boron oxidation in fluorine enriched environments.

Several general conclusions can be derived from the model results and analysis described in this report. They are:

(1) Re-evaluation of the B/H/O/C kinetics using the HBO heat of formation reported by Page[7], more recent reaction rate for the reaction of BO with O_2 (Stanton, et. al.)[18] and H_2 (Garland, et. al.)[19] and additional modeling results of Pasternack[20] resulted in an enhanced concentration of HBO as an intermediate. Additionally, B_2O_3 formation was found to be initiated earlier in the reaction sequence. Aside from these effects, there was no other significant change in the B/H/O/C chemistry from that found in earlier work.[1-3]

(2) Model results for several isothermal and adiabatic B/H/O/C/F systems have indicated that fluorine has a significant impact on the intermediate and product species distributions and the rate of energy release. The model results consistently show that OBF(g) is the major high temperature combustion product, whereas HBO_2(g) and B_2O_3(g) are the dominant reaction products in B/H/O/C systems. Both thermodynamic analysis and kinetic calculations suggest that with fluorine present at oxygen/fluorine mole ratios near unity, the post combustion gases will not consist of liquid B_2O_3. Further, comparisons with kinetic calculations for B/H/O/C systems suggest that the gas phase kinetics is as fast or faster with fluorine enrichment and that the heat release rate is increased.

(3) The most sensitive kinetic pathways have been identified. Fifteen fluorine-containing reactions have been identified for further theoretical and experimental

research. In addition, because OBF is a primary product in most of these reactions, research is needed on refining its heat of formation. The results also indicate that typical hydrocarbon combustion O/H chemistry remains important as well as many of reactions previously[1-3] identified as important kinetic pathways for B/H/O/C systems.

Efforts are currently underway to extend the gas phase kinetic model reported here by developing a model for heterogeneous chemistry associated with boron particle surface oxidation in fluorine enriched environments.

7.0 REFERENCES

1. Yetter, R.A., S.Y. Cho, H. Rabitz, Dryer, F.L., Brown, R.C. and Kolb, C.E., Chemical Kinetic Modeling with Sensitivity Analyses for Boron Assisted Hydrocarbon Combustion," Twenty-Second Symposium (International) on Combustion, p. 919, The Combustion Institute (1988).

2. Yetter, R.A., Rabitz, H., Dryer, F.L., Brown, R.C. and Kolb, C.E., "Kinetics of High Temperature B/O/H/C Chemistry," Combustion and Flame 83, 43 (1991).

3. Brown, R.C., Kolb, C.E., Cho., S.Y., Yetter, R.A., Rabitz, H. and Dryer, F.L., "Kinetics of High Temperature, Hydrocarbon Assisted Boron Combustion," in Gas-Phase Metal Reactions, A. Fontijn, Editor, Elsevier Science Publishers B.V., The Netherlands, in press (1992).

4. Brown, R.C., Kolb, C.E., Rabitz, H., Cho., S.Y., Yetter, R.A. and Dryer, F.L., "Kinetic Model of Liquid B_2O_3 Gasification in a Hydrocarbon Combustion Environment: I. Heterogeneous Surface Reactions," Int. J. Chem. Kinetics 23, 957 (1991).

5. Brown, R.C., Kolb, C.E., Cho, S.Y., Yetter, R.A., Rabitz, H. and Dryer, F.L., "Kinetic Model for Hydrocarbon Assisted Particulate Boron Combustion," in press Int. J. Chem. Kinetics, 1993.

6. Lawrence, B. private communication.

7. Page, M., "Multireference Configuration Interaction Study of the Reaction H_2 + BO -> HBO," J. Phys. Chem. 93, 3693 (1989).

8. Hills, A.J. and Howard, C.J., "Rate Coefficient Temperaturature Dependence and Branching Rates for the OH + ClO Reaction," J. Chem. Phys. 81, 4458 (1984).

9. JANAF Thermochemical Tables, Third Edition, Parts I and II. J. of Phys. and Chem. Ref. Data, Volume 14 (1985).

10. Light, G.C., Herm, R.R. and Matsumoto, J.N., "Rate Coefficients for the Reactions of BF with O and O_2," Chem. Phys. Lett. 70, 366 (1980).

11. Light, G.C., Herm, R.R. and Matsumoto, J.N., "Kinetics of Some Gas-Phase Elementary Reactions of Boron Monofluoride," J. Phys. Chem. 89, 5066 (1985).

12. Wolfhard, H.G., Draper, J.S., Riger, T.J. and Kolb, C.E., "Determination of the Infrared Emissions of Rocket Plumes and their Emitting Species," IDA paper P-1117, Institute for Defense Analysis, June, 1975.

13. DiGiuseppe, T.G. and Davidovits, P, "Boron Atom Reactions. II. Rate Constants With O_2, SO_2, CO_2 and H_2O," J. Chem. 74, 3287 (1981).

14. DiGiuseppe, T.G., Estes, R. and Davidovits, P., "Boron Atom Reactions and Rate Constants with H_2O, H_2O_2, Alcohols and Ethers," J. Phys. Chem. 86, 260 (1982).

15. Llewellyn, I.P., Fontijn, A. and Clyne, M.A.A., "Kinetics of the Reaction BO + O_2 ---> BO_2 + O," Chem. Phys. Lett. 84, 504 (1981).

16. Oldenborg, R.C. and Baughcum, S.L., "Gas Phase Oxidation of Boron Compounds," Abstracts of the 1986 AFOSR/ONR Contractors Meeting on Combustion, pg. 57, June, 1986.

17. Oldenborg, R.C. and Baughcum, S.L., "Gas-Phase Oxidation of Atomic Boron and Boron Monoxide," in Advances in Laser Science-I, Proceedings of the First International Laser Science Conferences, Dallas, Tx, 1985.

18. Stanton, C. T. Garland, N.L., and Nelson, H.H., "Temperature Depdendence of the Kinetics of the Reaction BO+O_2,", J. Phys. Chem. 95, 8741 (1991).

19. Garland, N.L., "Kinetic Studies of Boron and Aluminum Species," in Gas-Phase Metal Reactions, A. Fontijn, Editor, Elsevier Science Publishers B.V., The Netherlands, in press (1992).

20. Pasternak, Louise, "Gas Phase Modeling of Homogeneous Boron/Oxygen/ Hydrogen/Carbon Combustion," submitted Combustion and Flame.

21. Yetter, R.A., Dryer, F.L., and Rabitz, H.R., Combust. Sci. Tech. 79, 97 (1991).

22. Kee. R.J., Miller, J.A. and Jefferson, T.H., "CHEMKIN: A General Purpose, Problem Independent, Transportable Fortran Kinetics Code Package," Sandia National Laboratories Report SAND 80-8003, Livermore, CA, 1980.

23. Lutz, A.E., Kee. R.J. and Miller., J.A., SAND 87-8248, Sandia National Laboratories, Livermore, CA.

24. DASAC, Code for solving differential/algebraic equations distributed by Sandia National Laboratories, Livermore, CA.

25. Kramer, M.A., Calo, J.M., Rabitz, H and Kee, R.J., Sandia National Laboratories report SAND 82-8231, Livermore, CA., 1982.

26. Hindmarsh, A.C., ACM Sigum Newslett. 15(4) (1980).